Analysis of Functional Coupling: Mitochondrial Creatine Kinase and Adenine Nucleotide Translocase

Marko Vendelin,*† Maris Lemba,† and Valdur A. Saks*‡

*Laboratory of Fundamental and Applied Bioenergetics, Institut National de la Santé et de la Recherche Médicale E0221, Joseph Fourier University, Grenoble, France; †Institute of Cybernetics, Tallinn Technical University, Tallinn, Estonia; and ‡Laboratory of Bioenergetics, National Institute of Chemical Physics and Biophysics, Tallinn, Estonia

ABSTRACT The mechanism of functional coupling between mitochondrial creatine kinase (MiCK) and adenine nucleotide translocase (ANT) in isolated heart mitochondria is analyzed. Two alternative mechanisms are studied: 1), dynamic compartmentation of ATP and ADP, which assumes the differences in concentrations of the substrates between intermembrane space and surrounding solution due to some diffusion restriction and 2), direct transfer of the substrates between MiCK and ANT. The mathematical models based on these possible mechanisms were composed and simulation results were compared with the available experimental data. The first model, based on a dynamic compartmentation mechanism, was not sufficient to reproduce the measured values of apparent dissociation constants of MiCK reaction coupled to oxidative phosphorylation. The second model, which assumes the direct transfer of substrates between MiCK and ANT, is shown to be in good agreement with experiments—i.e., the second model reproduced the measured constants and the estimated ADP flux, entering mitochondria after the MiCK reaction. This model is thermodynamically consistent, utilizing the free energy profiles of reactions. The analysis revealed the minimal changes in the free energy profile of the MiCK-ANT interaction required to reproduce the experimental data. A possible free energy profile of the coupled MiCK-ANT system is presented.

INTRODUCTION

In muscle and brain cells, phosphocreatine and adenylate kinase shuttles provide a link between ATP-producing and ATP-consuming sites (Bessman and Geiger, 1981; Wallimann et al., 1992; Saks and Ventura-Clapier, 1994; Joubert et al., 2002, 2004; Dzeja and Terzic, 2003). As a part of phosphocreatine shuttle, the functional coupling between mitochondrial creatine kinase (MiCK) and adenine nucleotide translocase (ANT) has been identified by stimulating oxidative phosphorylation with creatine (Cr) (Bessman and Fonyo, 1966) and has been further examined with kinetic and structural studies (Jacobus and Lehninger, 1973; Saks et al., 1975; Seppet, 1979; Gellerich and Saks, 1982; Barbour et al., 1984; Wallimann et al., 1992). Recently, it has been shown that the coupling plays an important role in preventing the opening of the permeability transition pore and, thus, is critical for cell life (Dolder et al., 2003). However, regardless of the large amount of experimental data on functional coupling between MiCK and ANT dating back to the 1970s, the intimate mechanism of the interaction between the proteins is still not clear.

There are two mechanisms suggested to explain the effective interaction between MiCK and ANT: 1), the dynamic compartmentation of ATP and ADP (Gellerich et al., 1987) and 2), the direct transfer of ATP and ADP between the proteins (Saks et al., 1975; Jacobus and Saks, 1982). According to the first mechanism, functional coupling between MiCK and ANT can be explained by differences between the concentrations of ATP and ADP in intermembrane space and those in the surrounding solution due to some limitation of their diffusion across the outer mitochondrial membrane (Gellerich et al., 1987). According to the second mechanism of coupling, ATP and ADP are directly transferred between MiCK and ANT without leaving the complex of proteins (Jacobus and Saks, 1982). Neither of the proposed mechanisms have been checked quantitatively against the experimental measurements by thermodynamically consistent models that incorporate all the basic types of available data. Dynamic compartmentation hypothesis was used either to fit a limited set of experimental data (Gellerich et al., 1987) or applied in the development of several simplified phenomenological models of MiCK-ANT coupling used as part of models of intracellular energy transfer (Aliev and Saks, 1997; Vendelin et al., 2000b; Saks et al., 2003). The direct channeling has been analyzed mathematically by Aliev and Saks (1993, 1994) using a probability approach. In the two latter works, to simulate the measured alterations in the kinetics of MiCK reaction brought about by oxidative phosphorylation, the dissociation of ATP from its ternary complex with MiCK and Cr (*CK.ATP.Cr*) was not allowed in the model, i.e., this complex was always utilized in the MiCK reaction. A thermodynamically consistent analysis of the mechanism was not included in Aliev and Saks (1993, 1994), and is still absent.

The aim of this work is to identify the simplest mechanism able to reproduce the available experimental data on

Submitted October 29, 2003, and accepted for publication March 9, 2004.

Address reprint requests to Marko Vendelin at his present address: Laboratory of Fundamental and Applied Bioenergetics, INSERM E0221, Université J. Fourier, BP 53, F-38041, Grenoble, France. Tel.: 372-620-4151; Fax: 372-620-4169; E-mail: markov@ioc.ee.

Marko Vendelin's address as of January 1, 2005, will be Marko Vendelin, Institute of Cybernetics, Akadeemia 21, 12618 Tallinn, Estonia.

0006-3495/04/07/696/18 $2.00

doi: 10.1529/biophysj.103.036210

functional coupling between MiCK and ANT. The following experimental results were analyzed by the mathematical models: 1), changes in the apparent kinetic properties of the MiCK reaction when coupled to oxidative phosphorylation (Jacobus and Saks, 1982; Saks et al., 1985); 2), competition between MiCK-activated mitochondrial respiration by the competitive ATP-regenerating system (Gellerich and Saks, 1982); and 3), studies of radioactively labeled adenine nucleotide uptake by mitochondria in the presence of MiCK activity (Barbour et al., 1984). The results show that the direct transfer of ATP and ADP between ANT and MiCK is involved in the phenomenon of functional coupling between the proteins. The possible free energy profile of the functionally coupled reactions is presented.

METHODS

To test the two hypotheses of functional coupling between mitochondrial creatine kinase (MiCK) and adenine nucleotide translocase (ANT)—i.e., dynamic compartmentation and direct transfer between the proteins—the corresponding mathematical models were composed. First, we describe a simple model of dynamic compartmentation. Next, the modeling strategy for simulating direct transfer between MiCK and ANT is given. Finally, the simulation protocol as well as numerical methods are described. Details of the model based on the direct transfer between MiCK and ANT are given in the Appendix.

Model of dynamic compartmentation

According to the dynamic compartmentation hypothesis, the functional coupling between MiCK and ANT occurs through high ATP and ADP concentrations either in an intermembrane space (Gellerich et al., 1987) or in a narrow-space microcompartment (i.e., a gap) between the proteins (Aliev and Saks, 1997). In this study, our model assumes that there is a difference in the concentrations between the compartment and surrounding solution. Basic principles underlying the model composition were as follows (Fig. 1 *A*):

1. ANT was assumed to translocate adenine nucleotides between the matrix space and the compartment.
2. MiCK was linked to ATP and ADP in the compartment, while interacting with Cr and PCr from the solution.
3. Diffusion between the compartment and solution was considered to be restricted.

Consequently, the amounts of adenine nucleotides were tracked in two distinct compartments: in the solution (marked by the index *s* following the abbreviation of the metabolites, ADP_s and ATP_s) and in the compartment (index *c*, ADP_c and ATP_c). PCr and Cr were present only in the solution.

The following reactions occurring in the solution containing isolated mitochondria were accounted for: MiCK reaction, ANT transport (with the steady-state rate equal to oxidative phosphorylation), pyruvate kinase (PK) reaction (if PK was added), and background ATPase activity. The changes in concentrations of ATP and ADP in solution ($[ATP_s]$ and $[ADP_s]$) and the compartment ($[ATP_c]$ and $[ADP_c]$) were described by the equations

$$\frac{d[ATP_c]}{dt} = (-\nu_{CK} + \nu_{ANT} + \nu_{difATP})\ F_{volume}, \quad (1)$$

$$\frac{d[ADP_c]}{dt} = (\nu_{CK} - \nu_{ANT} + \nu_{difADP})\ F_{volume}, \quad (2)$$

$$\frac{d[ATP_s]}{dt} = -\nu_{difATP} - \nu_{ATPase} + \nu_{PK}, \quad (3)$$

$$\frac{d[ADP_s]}{dt} = -\nu_{difADP} + \nu_{ATPase} - \nu_{PK}, \quad (4)$$

where the factor F_{volume} denotes the ratio of the volume of the solution to that of the compartment and ν_{CK}, ν_{ANT}, ν_{difATP}, ν_{difADP}, ν_{ATPase}, and ν_{PK} correspond to the rate of MiCK reaction, ATP export from the matrix to the compartment by ANT, diffusion of ATP and ADP between compartment and solution, residual ATPase in solution, and PK reaction, respectively. Diffusion of nucleotides was governed by

$$\nu_{difATP} = D_{ATP}([ATP_s] - [ATP_c]), \quad (5)$$

$$\nu_{difADP} = D_{ADP}([ADP_s] - [ADP_c]), \quad (6)$$

where D_{ATP} and D_{ADP} are exchange coefficients. The concentrations of Cr, PCr, Mg^{2+}, Pi, and phosphoenolpyruvate (if present) were fixed at the onset of the simulations and assumed to be essentially constant during the experiment. The differential equations governing the system were solved until steady-state values of the variables were obtained.

Adenine nucleotides are known to form complexes with magnesium ions Mg^{2+}, which are subjected to creatine kinase reaction, whereas only Mg^{2+}-free nucleotides are translocated by ANT. The concentrations of the Mg^{2+}-bound nucleotides ($MgATP_s$, $MgADP_s$, $MgATP_c$, and $MgADP_c$) and Mg^{2+} free forms ($fATP_s$, $fADP_s$, $fATP_c$, and $fADP_c$) were related to the total amount of nucleotides (ATP_c and ADP_s) as

$$[fATP_c] = \frac{[ATP_c]}{1 + [Mg^{2+}]/K_{DT}}, \quad (7)$$

$$[MgATP_c] = [ATP_c] - [fATP_c], \quad (8)$$

$$[fATP_s] = \frac{[ATP_s]}{1 + [Mg^{2+}]/K_{DT}}, \quad (9)$$

$$[MgATP_s] = [ATP_s] - [fATP_s], \quad (10)$$

$$[fADP_c] = \frac{[ADP_c]}{1 + [Mg^{2+}]/K_{DD}}, \quad (11)$$

$$[MgADP_c] = [ADP_c] - [fADP_c], \quad (12)$$

$$[fADP_s] = \frac{[ADP_s]}{1 + [Mg^{2+}]/K_{DD}}, \quad (13)$$

$$[MgADP_s] = [ADP_s] - [fADP_s], \quad (14)$$

where $[Mg^{2+}]$ is the concentration of free Mg^{2+}, and K_{DT} and K_{DD} are Mg^{2+} dissociation constants from MgATP and MgADP, respectively. Concentration $[Mg^{2+}]$ was assumed to depend only on the amount of total Mg^{2+}, Pi, and nucleotides in the solution.

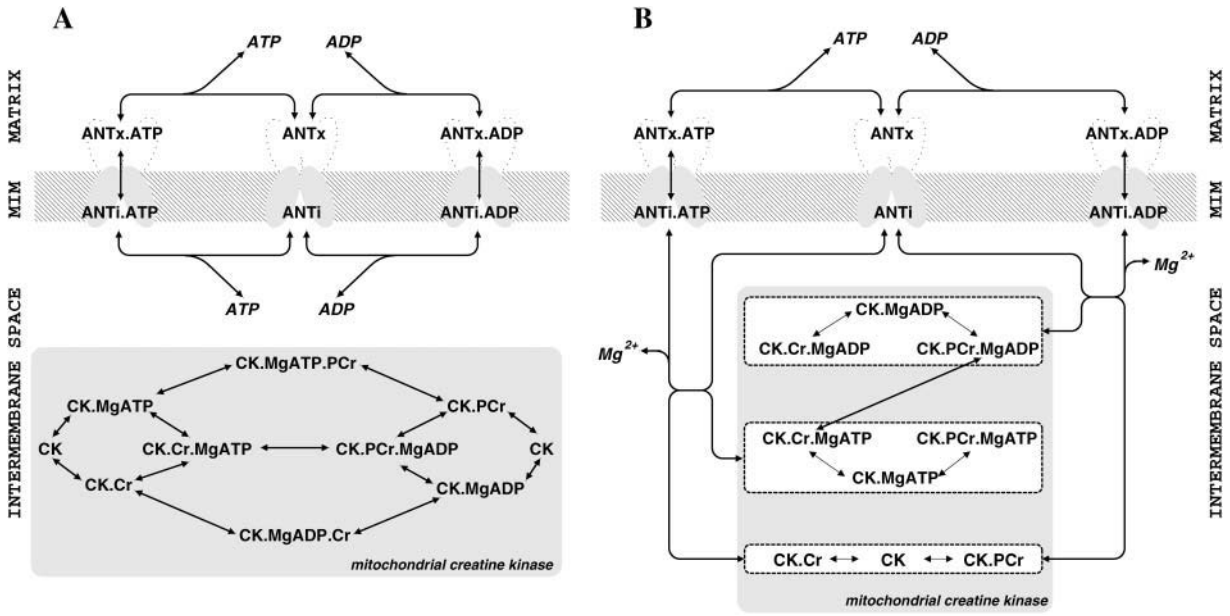

FIGURE 1 Scheme of interaction between mitochondrial creatine kinase (*MiCK*) and adenine nucleotide translocase (*ANT*). The interaction between the proteins is considered as a sum of two interaction modes: ATP and ADP are transferred through solution (*subplot A*) or directly channeled between the proteins (*subplot B*). In the model based on dynamic compartmentation hypothesis, only the interaction through solution is considered. When direct channeling between MiCK and ANT is assumed, both modes are taken into account. (*Subplot A*) In the first mode of MiCK-ANT interaction, ATP after transport from matrix to intermembrane space by ANT (link between ANTx.ATP and ANTi.ATP in the scheme) is released to solution. Next, the released ATP participates in MiCK reaction according to the random Bi-Bi mechanism with fast equilibrium between all states of MiCK. ADP produced by MiCK reaction is released into solution by MiCK and picked up by ANT for transport to mitochondrial matrix (link between ANTi.ADP and ANTx.ATP in the scheme). (*Subplot B*) In direct transfer mode, ATP is transferred from ANT to MiCK without leaving two-protein complex to solution. Since MiCK has only one binding site for ATP and ADP, such transfer is possible only if this site is free, i.e., MiCK is either free (*CK*) or has only Cr or PCr bound (*CK.Cr* and *CK.PCr*). In the scheme, we grouped the states of MiCK according to whether ATP or ADP is bound to enzyme or not (*open boxes* in the scheme with three states of MiCK in each group). During direct transfer of ATP from ANT to MiCK, MiCK is transferred from states CK, CK.Cr, and CK.PCr to states CK.MgATP, CK.Cr.MgATP, and CK.PCr.MgATP, respectively. In the scheme, this transfer is shown as a link between ANTi.ATP and two corresponding groups of MiCK states. Next, after MiCK reaction (link between states CK.Cr.MgATP and CK.PCr.MgADP in the scheme), ADP is transferred directly to ANT. Note, that MiCK operates with Mg-bound ATP and ADP and ANT requires Mg-free ATP and ADP forms. Thus, during direct transfer between MiCK and ANT, Mg is either bound or released, as shown in the scheme.

The rate equation of the MiCK reaction was derived according to the random-order Bi-Bi mechanism, assuming rapid equilibrium of substrate binding and product release (Jacobs and Kuby, 1970; Jacobus and Saks, 1982, Morrison and James, 1965),

$$\nu_{CK} = \left(\frac{V_{1CK}[MgATP_c][Cr]}{K_{icr}K_a} - \frac{V_{-1CK}[MgADP_c][PCr]}{K_{id}K_{cp}}\right)\Big/ Den_{CK}, \quad (15)$$

where

$$Den_{CK} = 1 + \frac{[Cr]}{K_{icr}} + \frac{[PCr]}{K_{icp}} + [MgATP_c]\left(\frac{1}{K_{ia}} + \frac{[Cr]}{K_{icr}K_a} + \frac{[PCr]}{K_{Icp}K_{ia}}\right) + [MgADP_c]\left(\frac{1}{K_{id}} + \frac{[PCr]}{K_{id}K_{cp}} + \frac{[Cr]}{K_{id}K_{Icr}}\right), \quad (16)$$

and $K_aK_{icr} = K_{ia}K_{cr}$, $K_dK_{icp} = K_{id}K_{cp}$. The constants V_{1CK}, V_{-1CK}, K_{ia}, K_a, K_{icr}, K_{id}, K_{icp}, K_{cp}, K_{Icp}, and K_{Icr} in the equations are the maximal forward and reverse rates of the MiCK reaction, and dissociation constants, respectively. According to the hypothesis of dynamic compartmentation, the constants were taken equal to those of the soluble MiCK. The indexes *a*, *cr*, *d*, and *cp* mark the dissociation of ATP, Cr, ADP, and PCr, respectively; these indexes correspond to the dissociation of a ternary complex and with an additional index *i* to the dissociation of the complex composed of MiCK and only one substrate. The parameters K_{Icp} and K_{Icr} are the dissociation constants of dead-end complexes.

Description of ANT kinetics was based on the phenomenological model by Korzeniewski (1998). The net rate of ATP export by ANT from the matrix to the compartment is described by the kinetic equations (Vendelin et al., 2000b)

$$\nu_{ANT}^{X\to G} = V_{ANT}\frac{[fADP_c]}{K_g + [fADP_c]} \times \left(\frac{[fADP_c]}{[fATP_c]e^{0.35\Delta\Psi/Z} + [fADP_c]} - \frac{[fADP_x]}{[fATP_x]e^{-0.65\Delta\Psi/Z} + [fADP_x]}\right), \quad (17)$$

where $[fATP_x]$ and $[fADP_x]$ are the concentrations of Mg^{2+}-free nucleotides in the matrix, K_g is the ANT reaction dissociation constant, $\Delta\Psi$ is the

membrane potential, and V_{ANT} is the maximal relative nucleotide transportation rate. Parameter Z is equal to RT/F, where R is the gas constant, T is the absolute temperature, and F is the Faraday number.

The residual ATPase activity ν_{ATPase} was characterized by the simple Michaelis-Menten equation of

$$\nu_{ATPase} = \frac{V_{ATPase}[ATP_s]}{[ATP_s] + K_{mx}}. \quad (18)$$

The formula for the pyruvate kinase reaction was obtained from Saks et al. (1984).

All values of the model parameters pertinent to the description of coupling between MiCK and ANT via dynamic compartmentation are given in Table 1.

Modeling strategy of direct transfer

To study the influence of direct transfer of ATP and ADP on MiCK kinetics, we composed the kinetic scheme of coupled ANT and MiCK reactions and investigated the free energy profiles of the reactions in detail, as explained below.

For simplicity, the following assumptions were made:

1. The concentrations of the substrates near ANT and MiCK were taken to be the same as the surrounding solution.
2. The total number of binding sites for ATP (ADP) on all MiCK and all ANT molecules is taken to be the same, with binding sites on MiCK molecules organized in pairs with the binding sites on ANT molecules. If one considers MiCK as an octamer, this may be taken to interact with the cluster of eight ANT dimers (Wallimann et al., 1992), with each ANT dimer having one binding site (Klingenberg, 1985).

No interactions were considered between molecules from different pairs. This allowed us to describe the state of coupled system by tracking only one binding site on ANT and one on MiCK, considerably simplifying the model.

TABLE 1 Parameters of the model of dynamic compartmentation

Parameter	Dimension	Value	Reference
K_{ia}	mM	0.75	Jacobus and Saks (1982)
K_a	mM	0.15	Jacobus and Saks (1982)
K_{cr}	mM	5.2	Jacobus and Saks (1982)
K_{icr}	mM	28.8	Jacobus and Saks (1982)
K_{id}	mM	0.205	Aliev and Saks (1993)
K_{icp}	mM	1.4	Aliev and Saks (1993)
K_{cp}	mM	0.5	Aliev and Saks (1993)
K_{Icr}	mM	28.8	Aliev and Saks (1993)
K_{Icp}	mM	35.0	Jacobus and Saks (1982)
V_{1CK}	s^{-1}	1.0	Aliev and Saks (1993)
V_{-1CK}	s^{-1}	4.2	Aliev and Saks (1993)
K_{DT}	mM	0.024	Vendelin et al., 2000b
K_{DD}	mM	0.347	Vendelin et al., 2000b
K_g	mM	0.005	Vendelin et al., 2000b
$fATP_x$	(relative)	4	Aliev and Saks (1993)
$fADP_x$	(relative)	1	Aliev and Saks (1993)
V_{ANT}	s^{-1}	1.0	
F_{volume}	(relative)	10^4	
K_{mx}	mM	0.98	Jacobus and Saks (1982)
$\Delta\Psi$	mV	–180	
F	J mol^{-1} mV^{-1}	96.5	
R	J mol^{-1} K^{-1}	8.3	
T	K	298.0	

The interaction between MiCK and ANT is considered as a sum of two interaction modes: 1), ATP and ADP are liberated into intermembrane space and then bound to MiCK or ANT or 2), directly channeled between the proteins. The first interaction mode is similar to that of the dynamic compartmentation, but without any diffusion restrictions after ATP or ADP release. Thus, when the proteins interact through ATP and ADP release and uptake from solution, ANT and MiCK reaction schemes are exactly the same as for the uncoupled system (see Fig. 1 *A*). In this case, ATP as well as all other substrates are in fast equilibrium with MiCK and the reaction follows the random Bi-Bi type mechanism. However, MiCK with no bound ATP or ADP molecule can also accept ATP (ADP) from ANT, which is transferred directly (see Fig. 1 *B*). In this case, we assume that when MiCK accepts ATP (ADP) from ANT directly, bound ATP and ADP cannot be in fast equilibrium with the surrounding solution. Thus, the equilibration of the MiCK binding site for ATP and ADP with the surrounding solution is prevented. For simplicity, we assumed that, in the case of direct transfer, MiCK is not exchanging ATP and ADP with solution at all, but returns ATP in the form of ADP or ATP back to ANT (Fig. 1 *B*). To distinguish the states of MiCK that are so tightly coupled to ANT from other MiCK states, an index c would be used in notations. For example, $CK_c.ATP$ would indicate the MiCK state with attached ATP received from ANT directly.

A thermodynamically consistent model was derived, taking into account the free energies of transition during each reaction as well as the principle of microscopic reversibility. This approach, based on the transition state theory of enzymatic reactions, allows one to study the free energy profile of the coupled system. In generalized form, the rates of monomolecular transition between two states of MiCK-ANT complex, noted as A and B, are governed by

$$\nu_+ = [A]\ \alpha\ e^{-(G^\ddagger - G_A)/RT}, \quad (19)$$

$$\nu_- = [B]\ \alpha\ e^{-(G^\ddagger - G_B)/RT}, \quad (20)$$

where ν_+ and ν_- are the rates of transitions between states A and B in forward and backward directions, respectively; $[A]$ and $[B]$ are normalized concentrations; α is a factor that depends on the nature of the transition; $G^\ddagger$ is a free energy in the transition state; G_A and G_B were the free energies of the states A and B, respectively; R is the gas constant; and T is the absolute temperature. Since in our further analysis we seek the overall rate constants and not the exact value of $G^\ddagger$ (see below), it is possible to predefine the value of α in the calculations. Using the free energy change $\Delta G_{A\to B} = G_B - G_A$ and the free energy of transition $\Delta G^\ddagger = G^\ddagger - G_A$, the rates ν_+ and ν_- would be

$$\nu_+ = [A]\ \alpha\ e^{-\Delta G^\ddagger/RT}, \quad (21)$$

$$\nu_- = [B]\ \alpha\ e^{-(\Delta G^\ddagger - \Delta G_{A\to B})/RT}. \quad (22)$$

The binding of the substrates to MiCK-ANT complex is modeled using similar equations, which are modified to take into account the bimolecular nature of the process. (For examples of these bimolecular reactions, see the equations following as well as the equations in the Appendix.)

Let us consider direct transfer of ATP from ANT to coupled MiCK, with the nucleotide binding site of the carrier directed toward intermembrane space and MiCK having no substrates bound. The process of ATP (ADP) transfer between ANT and MiCK is considered to be a conformational change within the MiCK-ANT complex. During this conformational change, a Mg^{2+} ion has to be attached, since MiCK reacts with the Mg-bound form of ATP only. The rate ν_+ of the transfer of ATP from ANT to MiCK and the rate for reverse transfer would be determined by the free energy of transition $\Delta G^\ddagger$ and the free energies of the participating substrates, which, in addition

to the free energies of ANT and MiCK complexes, includes the free energy of Mg^{2+} (G_{Mg}), as

$$\nu_+ = [ANTi.ATP - CK]\ [Mg^{2+}]\ \alpha\ \exp\left(\frac{-\Delta G^{\ddagger}}{RT}\right), \quad (23)$$

$$\nu_- = [ANTi - CK.ATP]\ \alpha\ \exp\left(\frac{-(\Delta G^{\ddagger} - \Delta G)}{RT}\right), \quad (24)$$

$$\Delta G = G_{\mathrm{ANTi-CK.ATP}} - G_{\mathrm{ANTi.ATP-CK}} - G_{\mathrm{Mg}}, \quad (25)$$

where [*ANTi.ATP-CK*] is the relative concentration of ANT and MiCK complex, with ANT directed toward intermembrane space and binding ATP, and substrate-free MiCK; [*ANTi-CK.ATP*] is the relative concentration of ANT and MiCK complex, with substrate-free ANT directed toward intermembrane space and MiCK forming a binary complex with ATP; and $G_{\mathrm{ANTi.ATP-CK}}$ and $G_{\mathrm{ANTi-CK.ATP}}$ are free energies of MiCK-ANT complex in states ANTi.ATP-CK and ANTi-CK.ATP, respectively.

To keep the number of model parameters as small as possible, we assumed that all transformations changing only a state of MiCK or ANT, depend on the participating states of this protein only. For example, according to this assumption, the rate of ATP binding from matrix to ANT does not depend on the state of MiCK. Thus, the respective rate of ATP binding should be specified in the model with only one $\Delta G^{\ddagger}$ and the free energies of ANT states involved without any dependence on MiCK state. The latter is achieved in the model by assuming that the free energy of the MiCK-ANT complex is a sum of the free energies of the ANT and MiCK states. For example, the free energies used in Eqs. 23–25 are $G_{\mathrm{ANTi.ATP-CK}} = G_{\mathrm{ANTi.ATP}} + G_{\mathrm{CK}}$ and $G_{\mathrm{ANTi-CK.ATP}} = G_{\mathrm{ANTi}} + G_{\mathrm{CK.ATP}}$.

In terms of the composed mathematical model, our aim is to find the values of the free energy of transition $\Delta G^{\ddagger}$ for every reaction between the states of the MiCK-ANT complex and the free energies of all states of the complex. In search for the simplest possible kinetic scheme of the coupling, we use the free energies of the enzyme and the carrier states as well as the $\Delta G^{\ddagger}$ estimated for an uncoupled system as much as possible. In the simplest possible model, only the $\Delta G^{\ddagger}$ for ATP and ADP binding with ANT would be changed, in addition to introducing the $\Delta G^{\ddagger}$ for direct transfer of ATP and ADP between the proteins. If this model fails to reproduce the measured data, then more parameters would be altered, until the minimal combination of changed parameters sufficient to reproduce the data is identified. This minimal combination of parameters would be the main result of our analysis. Naturally, this requires the parameters to be varied in a large range, before ruling a combination out as not sufficient to reproduce the experiment.

The system of equations for modeling the direct transfer between MiCK and ANT and values of the model parameters are described in the Appendix.

Protocol of simulations

There were two types of simulations performed in this study: 1), scanning of parameter space by changing specified model parameters independently from each other and 2), fitting the experimental data by minimization of residual function by variation of parameter values. Although analysis of the dynamic compartmentation comprised only the first type of simulation, both were employed in the direct transfer model.

In simulations with the dynamic compartmentation model, the values of maximal ATPase activity in the solution, ATP and ADP exchange constants D_{ATP} and D_{ADP}, were varied as follows: ATPase activity was varied from 0 to 17% of maximal MiCK activity in accordance with estimations of Jacobus and Saks (1982); exchange constants were varied from 10^{-10} s^{-1} to 10^{1} s^{-1}. During a scan in the model of direct transfer between MiCK and ANT, the free energies of the MiCK and ANT states were varied in a wide range from -15 kJ mol^{-1} to $+10$ kJ mol^{-1} and the free energies of transition were varied from 20 kJ mol^{-1} to 50 kJ mol^{-1} (corresponding to rate constants variation from ~0.002 s^{-1} to ~300 s^{-1}). The step sizes of these variations are specified for every simulation performed in the section Results.

When fitting the experimental data by the model, the residual function, subject to minimization, consisted of a sum of terms, each of which corresponded to one measurement: $((f_{\mathrm{exp}}-f_{\mathrm{cal}})/\sigma)^2$ with measured (f_{exp}) and computed (f_{cal}) rate (or apparent kinetic constant) and standard deviation (σ) of the measurements. To specify the dependence of the direction of MiCK reaction on oxidative phosphorylation (Saks et al., 1985), the following penalty term was added to all residual functions used in this study,

$$r = \begin{cases} 0, & \text{if } \nu_{\mathrm{CK}} \geq \varepsilon \\ (\gamma\ (\varepsilon - \nu_{\mathrm{CK}}))^2, & \text{if } \nu_{\mathrm{CK}} < \varepsilon \end{cases}, \quad (26)$$

where ν_{CK} is the MiCK reaction rate in the presence of oxidative phosphorylation and 4 mM PCr, 0.12 mM ATP, 0.05 mM ADP, and 40 mM Cr; ε was taken equal to 0.01 s^{-1}; and a large value $\gamma = 10^3$ was used to ensure that ν_{CK} remained larger than ε during optimizations.

In some experiments used, standard deviation (SD) was not reported, and the following approximations were used in this study:

1. MiCK reaction rates estimated from kinetic constants were assumed to have SD = 15% of the maximal rate of the MiCK reaction in the direction of PCr production.
2. Measurements of respiration rate after inhibition by the competitive ATP-regenerating system (Gellerich and Saks, 1982) were assumed to have SD = 10% of the respiration rate recorded without the competitive ATP-regenerating system in solution.
3. The estimation of the amount of ADP retransported to mitochondria after the MiCK reaction, without mixing with the surrounding solution (Barbour et al., 1984), was assumed to have the same SD at all ADP concentrations and to be equal to 10%.

The analysis of the direct transfer between MiCK and ANT was organized as follows:

1. The calculated solution was checked against the experimental data that required the smallest amount of simulations—i.e., dependence of MiCK reaction direction on the presence of oxidative phosphorylation in certain conditions (Saks et al., 1985).
2. All parameter values combinations that satisfied the first test were used to compute kinetic constants of MiCK reaction in the presence of oxidative phosphorylation.

The best 100 fits obtained during the second step were refined by minimizing the residual function using the selected fits as initial estimates of parameter values for minimization procedure, i.e., 100 optimizations were performed. The other two experiments considered in this study turned out to be readily reproducible with the combinations of parameter values passing the first two tests. Therefore, no further analysis was carried out.

Numerical methods

The system of ordinary differential equations was solved by the backward differentiation formula that is able to treat stiff equations (Brown et al., 1989). The accuracy of the solution was tested by varying the tolerance of the ordinary differential equation solver. The required optimization was performed using the Levenberg-Marquardt algorithm (Moré et al., 1984). The models were implemented using C++ and FORTRAN programming languages. The parts of C++ code for the model based on direct transfer hypothesis were generated by a Python script. Source code is available on request.

RESULTS

Dynamic compartmentation of ATP and ADP

According to the hypothesis of dynamic compartmentation, the concentrations of ADP and ATP in the compartment are different from those in the solution. This is due to the restricted diffusion of ATP and ADP between the solution and the compartment. The analysis of Eqs. 1–4 reveals that, in steady-state conditions, the sum of ATP and ADP concentrations in the compartment can differ from that in the solution only if the ATPase activity ν_{ATPase} is assigned a nonzero value. The latter can be demonstrated by taking the right side of the time-derivatives of Eqs. 1–4 equal to zero, reflecting the steady-state conditions. In that case, we obtain from Eqs. 3–6

$$-\frac{\nu_{ATPase}}{D_{ATP}} = [ATP_s] - [ATP_c], \quad (27)$$

$$\frac{\nu_{ATPase}}{D_{ADP}} = [ADP_s] - [ADP_c], \quad (28)$$

assuming that there is no pyruvate kinase in the solution ($\nu_{PK} = 0$). Adding Eqs. 27 and 28 results in

$$\nu_{ATPase}\left(\frac{1}{D_{ADP}} - \frac{1}{D_{ATP}}\right) = ([ATP_s] + [ADP_s]) - ([ATP_c] + [ADP_c]). \quad (29)$$

It becomes clear from Eq. 29 that the sum of ATP and ADP concentrations in the compartment can differ from the concentration in the solutions only if both of the following conditions are satisfied: 1), residual ATPase activity is present in the solution and 2), the values of ATP and ADP exchange constants are not equal to each other. Equation 29 also demonstrates that, to increase the total concentrations in the compartment, the term $(1/D_{ADP}–1/D_{ATP})$ should be negative and as large as possible by its absolute value, i.e., the exchange is fast for ADP and slow for ATP.

In Fig. 2, the apparent dissociation constants of ATP and Cr in MiCK reaction were computed as a function of ν_{ATPase} activity in the solution. In accordance with the analysis presented above, the exchange between solution and compartment was assumed to be fast for ADP and slow for ATP in these simulations. As Fig. 2, *A* and *B*, clearly demonstrates, increase of ATPase activity in the solution leads to a drop in computed apparent dissociation constants of ATP both from ternary and binary complexes with MiCK, K_a, and K_{ia}, respectively. However, the K_a and K_{ia} values that have been measured by Jacobus and Saks (1982) are reached by the model at different ν_{ATPase} activities (Fig. 2). Within the model, it is not possible to reproduce the experimentally observed 10-fold and 2.5-fold decreases in the values of soluble MiCK dissociation constants simultaneously with one parameter set. This can be demonstrated by computing K_a and K_{ia} at different combinations of ν_{ATPase}, D_{ATP}, and D_{ADP} values (Fig. 3). Indeed, the computed line, characterizing the relationship between K_a and K_{ia} values, does not

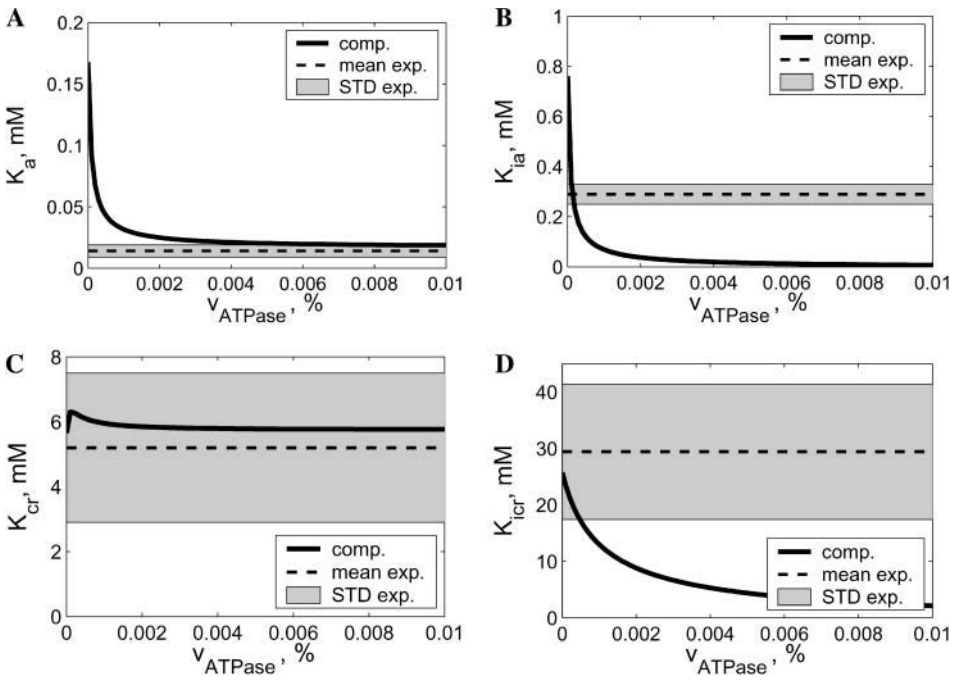

FIGURE 2 Calculated apparent dissociation constants of MiCK reaction as functions of ATPase activity (ν_{ATPase}) in the solution in the presence of oxidative phosphorylation. Coupling between MiCK and oxidative phosphorylation was modeled according to the dynamic compartmentation hypothesis. ATPase activity is presented relative to maximal MiCK activity, in percents. Subplots A, B, C, and D correspond to apparent K_a, K_{ia}, K_{cr}, and K_{icr}, respectively. The simulation results (*solid lines*) obtained with the model are compared with the measured values of apparent dissociation constants, indicated by the average measured value (*dashed line*) and shaded area corresponding to the measured average ± standard deviation (SD) (data from Jacobus and Saks, 1982). In the calculations, maximal activity of ANT was taken equal to that of MiCK; ATP and ADP exchange constants D_{ATP} and D_{ADP} were 10^{-9} s^{-1} and 10^{-1} s^{-1}, respectively. Note that with the increase of ATPase activity in the solution, apparent dissociation constants of ATP from ternary and binary complexes with MiCK (K_a and K_{ia}, respectively) are reduced considerably.

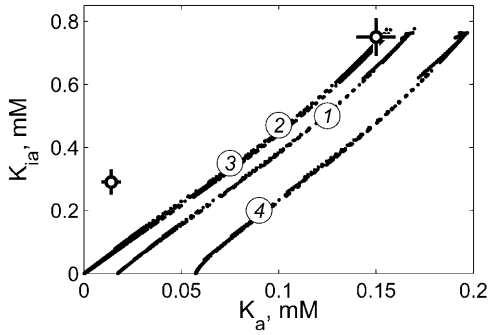

FIGURE 3 Calculated apparent dissociation constants K_a and K_{ia} of the MiCK reaction in the presence of oxidative phosphorylation. Coupling between MiCK and oxidative phosphorylation was modeled according to the dynamic compartmentation hypothesis. Here, apparent dissociation constants K_a and K_{ia} (represented by *small dots* in the figure) were computed in case of different combinations of the values of ATPase activity in the solution ν_{ATPase} and exchange constants D_{ATP} and D_{ADP}. In the figure, the measured values are shown (*open circles*) in the right upper corner (no oxidative phosphorylation) and in the left lower corner (with oxidative phosphorylation). When using the kinetic constants of ANT transport as given in Table 1, all combinations of computed K_a and K_{ia} are aligned along the line with index 1 (indexes are shown within *larger open circles* in the figure). By increasing the maximal activity of ANT by 10 or 100 times, this line can be shifted to the left (lines with indexes 2 and 3, respectively). When instead of increasing the maximal activity of ANT, the apparent dissociation constant K_g is increased, the line shifts to the right (line with index 4). Note that regardless of the values used of ANT kinetic constants, all computed combinations of K_a and K_{ia} were considerably adrift from the measured values of these constants in the presence of oxidative phosphorylation. Experimental data from Jacobus and Saks (1982).

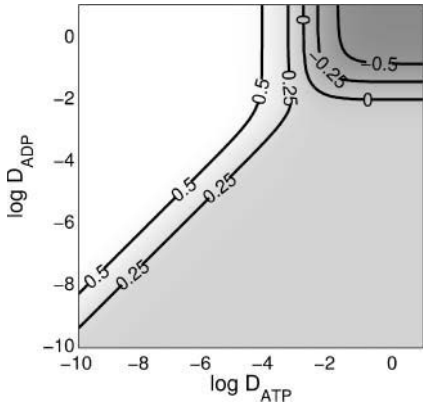

FIGURE 4 Analysis of the direction of the MiCK reaction in the presence of oxidative phosphorylation. In this contour plot, the rates of the MiCK reaction, relative to the maximal rate of the MiCK reaction in the direction of PCr synthesis, are depicted by different shades and iso-lines. Numbers on the iso-lines show the value of reaction rates; positive values correspond to PCr synthesis. The shades correspond to the values of MiCK reaction rate, changing gradually from white (*maximal rate*, *PCr synthesis*) to dark gray (*minimal rate*, *ATP synthesis*). Concentrations in solution were kept at the following values: 2 mM PCr, 0.12 mM ATP, 0.05 mM ADP, and 5 mM Pi. According to Saks et al. (1985), the direction of MiCK reaction depends on whether MiCK is coupled to oxidative respiration or not (Saks et al., 1975). Namely, whereas coupling of MiCK to oxidative phosphorylation favors the synthesis of PCr by MiCK (*positive reaction rates* on the figure), noncoupled MiCK reaction is driven toward the breakdown of PCr (*negative reaction rates* on the figure). D_{ATP} and D_{ADP} are exchange constants that characterize the exchange of ATP and ADP between the compartment and the solution (both constants are given in s^{-1}). Note that at smaller values of D_{ATP} and D_{ADP}, the MiCK reaction direction predicted by the model is in correspondence with the measurements (reaction rate is positive).

pass the point coordinates, which are the measured dissociation constant values in the presence of oxidative phosphorylation. This holds true regardless of the ATPase activity used and the values of the exchange constants in the wide range of values used. The increase of model ANT activity leads to the shift of the K_a–K_{ia} relationship toward the measured values to a certain limit. This limit is still adrift from the measurements (Fig. 3). We conclude from the results that the model based on dynamic compartmentation hypothesis is unable to reproduce the measurements. Due to such a strict relationship between computed values of K_a and K_{ia} there is no need to use minimization for fitting the experimental data to check this conclusion—altering parameter values is neither going to change the slope of the lines nor cross the limit obtained with the high ANT activities, as is evident from scanning the parameter space (Fig. 3).

The model was tested additionally in regard to the following two experiments: 1), the reversal of the MiCK reaction, coupled to oxidative phosphorylation, as opposed to the noncoupled MiCK in the case of nonrespiring mitochondria in the presence of 4 mM PCr, 0.12 mM ATP, 0.05 mM ADP, and 40 mM creatine Cr in solution (Fig. 4), and 2), inhibition of MiCK-activated mitochondrial respiration by the competitive ATP-regenerating system (Fig. 5). The conclusions drawn from these simulations did not depend on the ATPase activity in the solution. From the analysis of the results in Figs. 4 and 5, it is clear that both experiments can be reproduced by the same parameter values. Indeed, all combinations of D_{ATP} and D_{ADP} that lead to the positive MiCK reaction rates on Fig. 4 and to 60% drop of respiration rate, after addition of the ATP-regenerating system (iso-line with value ~0.4 on Fig. 5), are in agreement with these two experiments.

In sum, the model composed on the basis of the dynamic compartmentation hypothesis can reproduce the reversal of the MiCK reaction after coupling to oxidative phosphorylation in certain conditions (Fig. 4) and measured inhibition of MiCK-activated mitochondrial respiration by the competitive ATP-regenerating system (Fig. 5). However, the kinetics of the MiCK reaction coupled to oxidative phosphorylation cannot be reproduced with any combination of model parameters (Fig. 3), indicating that the alternative hypothesis of functional coupling between MiCK and ANT has to be considered to reproduce the measurements on isolated heart mitochondria.

Direct transfer of ATP and ADP between creatine kinase and adenine nucleotide translocase

The model of direct transfer of substrates between MiCK and ANT contains two important modifications if compared with

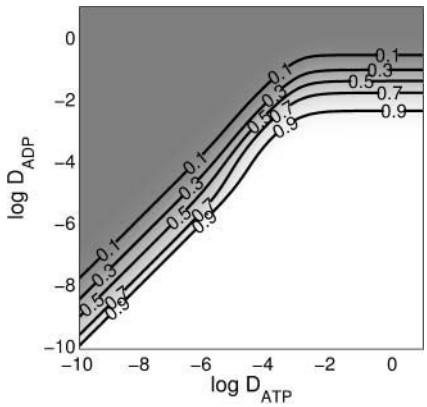

FIGURE 5 In this contour plot, the relative decrease in respiration rate after addition of the external ADP-trapping system into the solution containing isolated respiring mitochondria in the presence of oxidative phosphorylation is shown. The decrease v/v_0, where v_0 and v are the respiration rate before and after pyruvate kinase and phosphoenolpyruvate (PK+PEP) addition, is depicted by different shades and iso-lines. Numbers on the iso-lines show the value of v/v_0, shades change gradually from white ($v/v_0 = 1$, no drop in respiration) to dark gray ($v/v_0 = 0$, respiration completely inhibited). Initial conditions in the solution: 0.33 mM ATP, 0 mM ADP and PCr, 33 mM Cr, 5 mM Mg^{2+}, 10 mM Pi, and 2.5 mM PEP. In the calculations, the activity of PK+PEP system was taken to be infinite compared to that of MiCK. According to Gellerich and Saks (1982), PK+PEP system is able to decrease the rate of respiration by ~60% at maximum, i.e., the decrease v/v_0 is ~0.4. D_{ATP} and D_{ADP} are exchange constants that characterize the exchange of ATP and ADP between the compartment and the solution (both constants are given in s^{-1}). In these simulations, ATPase activity in the solution was taken to be equal to 0.1% of the maximal activity of MiCK. Varying ATPase activity did not alter the results qualitatively. Note that the region in D_{ATP}–D_{ADP} plane corresponding to the measured drop in respiration rate is rather limited (see area around $v/v_0 = 0.4$ in the figure).

the model based on the dynamic compartmentation hypothesis. First, the concentrations of the metabolites near MiCK and ANT are the same as in solution; i.e., there is no diffusion restriction separating the compartment from the surrounding solution. Second, ATP and ADP can be transferred directly between MiCK and ANT, in addition to transfer through solution.

Kinetics of creatine kinase reaction coupled to oxidative phosphorylation

In the direct transfer model, ADP and ATP release by MiCK-ANT complex into the solution was reduced and a link between MiCK and ANT was established. For that, free energies of transition $\Delta G^{\ddagger}$ corresponding to ATP (ADP) release to the solution and to direct transfer of ATP (ADP) between MiCK and ANT had to be specified. To investigate whether such changes would be sufficient for reproduction of the measured data on MiCK-ANT coupling, we varied the values of these $\Delta G^{\ddagger}$ in a wide range independently from each other and computed the rate of MiCK reaction coupled to oxidative phosphorylation, with 4 mM phosphocreatine (PCr), 0.12 mM ATP, 0.05 mM ADP, and 40 mM creatine (Cr) in solution. According to Saks et al. (1985), MiCK reaction is directed toward PCr synthesis (positive direction) in these conditions. However, regardless of the $\Delta G^{\ddagger}$ combinations used, the computed MiCK rate was always in the opposite direction. The computed MiCK reaction was positive when, in addition to the parameters mentioned above, at least one of the following parameters was varied: 1), the free energy of transition $\Delta G^{\ddagger}$ of the MiCK reaction coupled with ANT; 2), the free energy of ANT directed toward the intermembrane space with ATP attached; or 3), the free energies of the MiCK states coupled with ANT. In the last case, the free energy of CK_c.ATP was varied and the free energies of all other coupled MiCK states with bound ATP or ADP (Fig. 1 *B*) were computed to keep differences between the free energies of MiCK states the same as for similar states in isolated MiCK.

Next, we computed the apparent kinetic constants of the MiCK reaction in the presence of oxidative phosphorylation and compared these with the measured data (Jacobus and Saks, 1982). The apparent kinetic constants were computed only for such combinations of parameter values as would reproduce the measured direction of the MiCK reaction as described above (i.e., that would satisfy the criteria in the following text and tables). To check whether direct transfer of metabolites between MiCK and ANT allows us to overcome the difficulties of modeling the MiCK reaction kinetics encountered using the dynamic compartmentation hypothesis (Fig. 3), we plotted all computed apparent dissociation constants K_a and K_{ia} against each other in a diagram (Fig. 6). As made clear from the figure, the region with the measured values of K_a and K_{ia} is covered by the model solution, and it is possible to find a combination of model parameters that would lead to the measured combination of K_a and K_{ia}

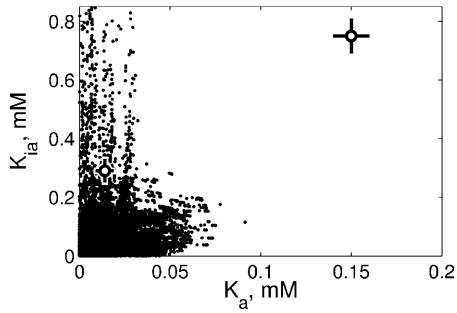

FIGURE 6 Calculated apparent dissociation constants K_a and K_{ia} of the MiCK reaction in the presence of oxidative phosphorylation. Coupling between MiCK and oxidative phosphorylation was modeled assuming direct transfer of metabolites between ANT and MiCK. Apparent dissociation constants K_a and K_{ia} (represented by *small dots* in the figure) are computed for different combinations of the free energies of the MiCK-ANT complex states and the free energies of transition. In the figure, the measured values are shown by open circles in the right upper corner (no oxidative phosphorylation) and in the left lower corner (with oxidative phosphorylation). Note that the range of computed K_a–K_{ia} combinations covers the area near the measured values of these constants in the presence of oxidative phosphorylation. Experimental data from Jacobus and Saks (1982).

values. The best fits obtained by the model during such independent variation (denoted by *scan*) for different varied parameter sets as well as the results of model fitting simulations (see below) are summarized in Table 2. Note that in some cases the computed kinetic constants were negative. This is due to the procedure used to calculate kinetic constants from the computed MiCK reaction rate (the same as in Jacobus and Saks, 1982), and clearly indicates that the model cannot reproduce the measured data with the corresponding set of parameters.

We refined the results either by fitting the measured kinetic constants directly (simulation *OKm* in Table 2) or by fitting the MiCK reaction rate estimated from the measured kinetic constants (simulation *OVel* in Table 2). These two simulations were performed to ensure that not only could apparent kinetic constants be fitted (*OKm*), but that estimated MiCK reaction rates at all concentration combinations could be used in the experiment as well (*OVel*). According to the results presented in Table 2, the model was able to reproduce the measured kinetic constants only if the free energy of

TABLE 2 Apparent kinetic constants of creatine kinase reaction coupled to oxidative phosphorylation

	Varied parameters, step size														
	Free energy of activation $G^{\ddagger}$, kJ mol^{-1}														
	N_i.T ↕	N_i.D ↕	N_i.T ↕	N_i.D ↕	CK_c.T.Cr ↕	Free energy, kJ mol^{-1}			Computed kinetic constants						
	CK_c.T	CK_c.D	*sol*	*sol*	CK_c.D.PCr	N_i.T	N_i.D	CK_c	K_{ia} mM	K_a mM	K_{icr} mM	K_{cr} mM	K_{Icp} mM	K_{icp} mM	V_1s^{-1}	
scan	1.0	1.0	1.0	1.0					**No combination satisfied the criterion**							–
scan	2.0	2.0	2.0	2.0	2.0				**0.20**	**−0.007**	**−10.0**	**0.36**	**0.94**	**0.056**	0.98	–
OKm	*	*	*	*	*				0.28	**−0.005**	**−14.9**	**0.26**	**0.94**	**0.077**	0.96	–
OVel	*	*	*	*	*				**0.13**	0.011	29.8	2.5	**1.6**	**0.65**	0.95	–
scan	2.0	2.0	2.0	2.0		2.5			**0.12**	0.017	36.5	5.2	10.8	1.1	0.89	+
OKm	*	*	*	*		*			**0.15**	0.016	40.2	4.2	10.3	1.3	0.94	+
OVel	*	*	*	*		*			**0.12**	0.018	35.8	5.2	11.0	1.1	0.90	+
scan	1.5	1.5	1.5	1.5			1.5		**No combination satisfied the criterion**							
scan	2.0	2.0	2.0	2.0				2.5	0.32	**−0.007**	**1.2**	**−0.028**	**1.4**	1.3	**0.084**	–
OKm	*	*	*	*				*	**0.002**	0.004	**2.0**	3.4	**1.5**	**2.0**	**0.46**	–
OVel	*	*	*	*				*	**0.066**	0.011	21.5	3.4	**2.5**	**0.66**	**0.62**	–
scan	3.0	3.0	3.0	3.0		4.0	4.0		**0.12**	0.020	32.6	5.3	11.4	1.3	0.92	+
OKm	*	*	*	*		*	*		**0.12**	0.018	37.2	5.4	17.7	1.4	0.93	+
OVel	*	*	*	*		*	*		**0.12**	0.021	31.9	5.3	11.3	1.3	0.92	+
scan	3.0	3.0	3.0	3.0		4.0		4.0	0.23	0.022	**57.0**	5.4	37.8	1.0	0.81	+
OKm	*	*	*	*		*		*	0.23	0.023	50.6	5.2	17.2	1.3	0.89	+
OVel	*	*	*	*		*		*	**0.13**	0.019	35.4	5.2	14.5	1.1	0.91	+
scan	3.0	3.0	3.0	3.0	3.0			4.0	0.32	**−0.013**	**−3.4**	**0.14**	**0.19**	**0.28**	0.80	–
OKm	*	*	*	*	*			*	0.30	**−0.006**	**−7.3**	**0.14**	**0.21**	**0.26**	0.90	–
OVel	*	*	*	*	*			*	0.22	0.009	**61.5**	2.5	**1.5**	**0.88**	1.0	–
scan	3.0	3.0	3.0	3.0		5.0	5.0	5.0	0.26	**0.025**	**55.3**	5.2	15.0	1.4	0.89	–
OKm	*	*	*	*		*	*	*	0.24	0.023	52.9	5.2	23.8	1.4	0.88	+
OVel	*	*	*	*		*	*	*	**0.15**	0.021	37.6	5.3	22.1	1.5	0.89	+
scan	3.0	3.0	3.0	3.0	3.0	5.0	5.0	5.0	0.24	0.018	**68.0**	5.0	18.2	**0.93**	0.83	–
OKm	*	*	*	*	*	*	*	*	0.26	0.024	52.1	4.8	18.2	1.3	0.91	+
OVel	*	*	*	*	*	*	*	*	0.22	**0.025**	43.0	4.8	9.0	1.5	1.00	+
									Measured kinetic constants (Jacobus and Saks, 1982)							
								Mean	0.29	0.014	29.4	5.2	~20–50	1.4	0.93	
								SD	±0.04	±0.005	±12	±2.3		±0.2	±0.1	

In the table, simulations corresponding for the same combination of varied parameters are grouped. We varied the following free energies in simulations: $\Delta G^{\ddagger}$ of ATP transfer between ANT and MiCK (denoted by $N_i.T \leftrightarrow CK_c.T$ in the table), $\Delta G^{\ddagger}$ of ADP transfer between ANT and MiCK ($N_i.D \leftrightarrow CK_c.D$), $\Delta G^{\ddagger}$ of ATP or ADP release from ANT to solution ($N_i.T \leftrightarrow sol$ and $N_i.D \leftrightarrow sol$, respectively), $\Delta G^{\ddagger}$ of MiCK reaction coupled to ANT ($CK_c.T.Cr \leftrightarrow CK_c.D.PCr$), free energy of ANT directed to intermembrane space with either ATP or ADP attached ($N_i.T$ and $N_i.D$, respectively), and free energies of MiCK states with ATP or ADP received from ANT through direct transfer (CK_c). The right part of the table shows the best fit for each series of simulations. The type of simulation is indicated in the first column: ''scan'' corresponds to independent variation of parameters; in *OKm* and *OVel* the measured kinetic constants or estimated MiCK reaction rate were fitted by the model, respectively. In the case of independent variation of parameters, the step size used during a scan is indicated in the table. For simulations *OKm* and *OVel*, the optimized parameters are indicated by *. The computed values are presented in bold typeface, if >2 SDs adrift from the values measured by Jacobus and Saks (1982) (see the bottom of the table); otherwise regular typeface was used. A simulation, rendering more than one computed kinetic constant that was far from the measured value, was considered as a failed one and marked by − in the last column of the table. The rest of the simulations were considered to have passed the test and marked by + in the last column of the table.

ANT directed to the intermembrane space with attached ATP (N_i.T) was varied. The fit became better if more parameters were varied in addition to the variation of N_i.T free energy, with the best fits obtained in the last two combinations of varied parameters (see Table 2, simulations *OKm* and *OVel*).

ADP flux between creatine kinase and adenine nucleotide translocase

We analyzed further those parameter combinations able to reproduce the MiCK reaction rate kinetics relatively well. For this analysis, in addition to the experimental data on the kinetics of the MiCK reaction coupled to oxidative phosphorylation, we analyzed ADP flux between MiCK and ANT. In our simulations, the model was used to reproduce the following experimental data:

1. Rate of MiCK reaction coupled to oxidative phosphorylation, estimated from apparent kinetic constants (Jacobus and Saks, 1982).
2. Inhibition of MiCK-activated mitochondrial respiration by the competitive ATP-regenerating system (Gellerich and Saks, 1982).
3. Studies of radioactively labeled adenine nucleotide uptake by mitochondria in presence of MiCK activity (Barbour et al., 1984).

The best fits, obtained using the same set of initial estimates as in the simulations *OKm* and *OVel* in Table 2, are presented in Table 3 and Figs. 7–9. These results are analyzed below.

The computed kinetic constants of MiCK reaction in the presence of oxidative phosphorylation are demonstrated in Table 3. In Table 3, we numbered parameter combinations (*first column* in the table) and used exactly the same notations as in Table 2. Since in this analysis we fitted not only the kinetics of the MiCK reaction but other experiments as well, computed kinetic constants are further adrift from the experimental data than the results presented in Table 2. However, when the computed MiCK rate is compared with the MiCK rate estimated from measured kinetic constants, it is clear that the difference between these two rates is relatively small (see Fig. 7 *A*). According to Fig. 7 *A*, the computed MiCK reaction rate underestimates the measured values in simulation *3* and, at high PCr concentration, in simulation *1*. Such behavior of the model solution is also clear from the results presented in Table 3. Namely, the computed maximal rate of MiCK reaction V_1 in simulation *3* was smaller than that actually measured and, due to the relatively small apparent inhibition constant K_{icp} in simulation *1*, PCr inhibition of the MiCK reaction rate is more profound in the simulations than in the measurements. To test the model, we repeated the simulations with inhibited oxidative phosphorylation and obtained a MiCK rate close to that actually measured (Fig. 7 *B*).

According to our simulations (Fig. 8), the computed inhibition of oxidative phosphorylation by the competitive ATP-regenerating system (PK+PEP) was close to the results of measurements by Gellerich and Saks (1982). Additionally, the model was able to reproduce the competition between ADP supplied by the coupled MiCK reaction and ADP from solution estimated from radioactively labeled adenine nucleotide uptake by mitochondria (Fig. 9). Namely, the computed amount of adenine nucleotides that were retransported to mitochondria without mixing with surrounding solution is close to the estimations by Barbour et al. (1984). In sum, the model was able to reproduce an estimated competition between ADP sources and inhibition of respiration by pyruvate kinase with all combinations of varied parameters that reproduced kinetic measurements of the MiCK reaction (Jacobus and Saks, 1982; Saks et al., 1985).

Free energy profile of coupled MiCK-ANT reaction

The free energy profiles of the MiCK reaction estimated for the uncoupled case and that coupled to ANT are presented

TABLE 3 Apparent kinetic constants of creatine kinase reaction coupled to oxidative phosphorylation

	Varied parameters, step size													
	Free energy of activation $G^{\ddagger}$, kJ mol^{-1}													
	N_i.T ↕	N_i.D ↕	N_i.T ↕	N_i.D ↕	CK_c.T.Cr ↕	Free energy, kJ mol^{-1}			Computed kinetic constants					
	CK_c.T	CK_c.D	*sol*	*sol*	CK_c.D.PCr	N_i.T	N_i.D	CK_c	K_{ia} mM	K_a mM	K_{icr} mM	K_{cr} mM	K_{Icp} mM	K_{icp} mM	V_1s^{-1}
1	*	*	*	*		*			**0.085**	0.018	26.1	5.5	19.4	**0.71**	0.83
2	*	*	*	*		*	*		**0.11**	0.023	24.6	5.3	26.6	1.4	0.84
3	*	*	*	*		*		*	**0.16**	**0.032**	25.7	5.2	17.3	1.1	0.77
4	*	*	*	*		*	*	*	**0.11**	0.021	28.1	5.4	27.4	1.3	0.84
5	*	*	*	*	*	*	*	*	**0.17**	**0.028**	29.9	4.8	24.6	1.4	0.94
									Measured kinetic constants (Jacobus and Saks, 1982)						
								Mean	0.29	0.014	29.4	5.2	~20–50	1.4	0.93
								SD	±0.04	±0.005	±12	±2.3	—	±0.2	±0.1

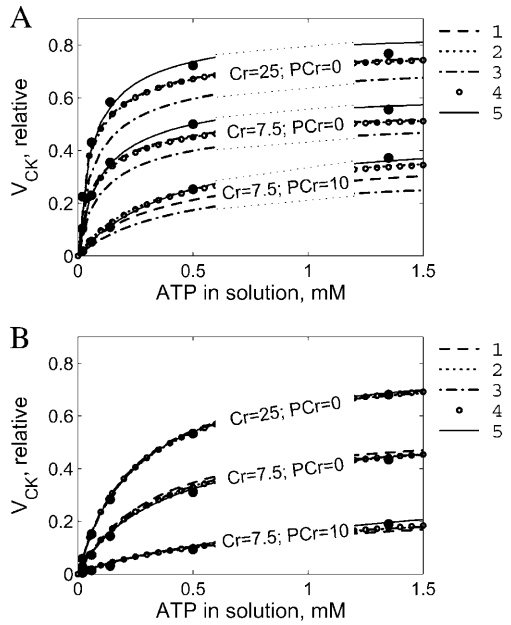

FIGURE 7 Computed MiCK reaction rate as a function of ATP with (*subplot A*) and without (*subplot B*) oxidative phosphorylation. Coupling between MiCK and oxidative phosphorylation was modeled assuming direct transfer of metabolites between ANT and MiCK. (*Subplot A*) Experimental data (*black dots*) was reproduced by model with five different parameter sets. The parameter sets are indexed (see Table 3); correspondence between line-type and the index is shown in the legend. In this subplot, the MiCK reaction rate is shown for ATP titrations in the presence of three different combinations of Cr and PCr concentrations, which are indicated in the figure in mM. Note that all used parameter sets fit experimental data quite well, with parameter set *3* somewhat underestimating the reaction rate. (*Subplot B*) Computed MiCK rate with inhibited oxidative phosphorylation is in correspondence with the experimental data (*black dots*). The same parameter sets were used as in subplot A. Experimental MiCK rate used in both subplots was estimated on the basis of apparent MiCK reaction kinetic constants reported in Jacobus and Saks (1982).

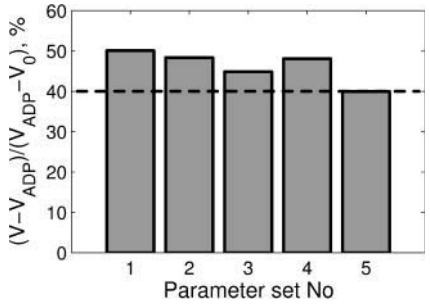

FIGURE 8 Inhibition of respiration rate by a concurrent enzyme system, 60 IU/ml pyruvate kinase and phosphoenolpyruvate (*PEP*). The respiration was stimulated by the addition of 0.33 mM of ADP in the presence of 33 mM Cr. In the figure, the respiration rate after addition of PK+PEP (*V*) is normalized by the respiration rate obtained before PK+PEP addition (V_{ADP}), as shown in the *y*-axis label (V_0 corresponds to the respiration rate without added ADP). The simulation results (*bars*) are compared with the measured drop in VO_2, indicated by the average measured VO_2 (*dashed line*). The parameter sets are indexed (Table 3). Note that results obtained with all parameter sets used are close to the measurements. Experimental data is from Gellerich and Saks (1982).

in Fig. 10, parts *A* and *B*, respectively. The following predictions can be drawn from our analysis of MiCK reaction coupled to ANT.

First, the free energies of the states with ATP^{4-} attached to ANT (*left column* in the scheme in Fig. 10 *B*) are considerably larger than in the case of the uncoupled system. For the uncoupled system, the attachment of Mg-free ATP^{4-} from solution by ANT leads to the drop of total free energy by 13.13 kJ mol^{-1} (see Appendix, Parameter Values, and *boxes with the dashed border* in Fig. 10 *B*). However, in the free energy profile found by our fitting for the coupled system, the attachment of Mg-free ATP^{4-} from solution by ANT (transition from state CK+T to CK-Ni.T in the scheme) leads to increase of the free energy indicating an elevation of free energies of MiCK-ANT complex with ATP^{4-} attached to ANT_i in comparison with the uncoupled system. Due to such elevation of the free energy, the transfer of ATP^{4-} from ANT to MiCK becomes energetically advantageous (compare the free energies of the states in the *left column* and in the *middle column* of the scheme). In addition to the elevated free energy of the MiCK-ANT complex with ATP^{4-} attached to ANT_i, the attachment of magnesium during the transfer of ATP^{4-} from ANT_i to coupled MiCK decreases the free energy by 7.44 kJ mol^{-1}. Thus, the elevation of the free energy of the MiCK-ANT complex with ATP^{4-} attached to ANT_i and the attachment of magnesium facilitates the direct transfer of ATP^{4-} from ANT to MiCK.

Second, in line with the changes of the free energy of the coupled MiCK-ANT complex with ATP^{4-} attached to ANT_i (*left column* in the scheme), the free energy of the complex with ADP^{3-} attached to ANT_i is slightly lower than in the uncoupled system (*right column* in the scheme). This is clear from inspecting the difference between states CK+D and CK-Ni.D in the scheme (compare the free energies for coupled and uncoupled cases in Fig. 10 *B*).

Thus, the free energies of MiCK-ANT complex before the transfer of ATP^{4-} to MiCK are considerably elevated

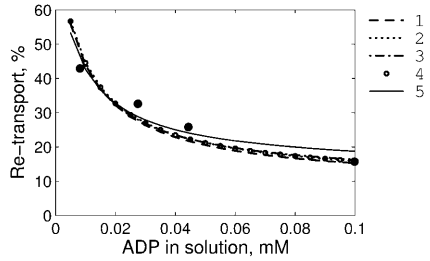

FIGURE 9 Competition between ADP supplied by MiCK reaction and ADP from solution. The amount of ADP retransported to mitochondria after MiCK reaction, without mixing with ADP in the intermembrane space, is shown at different levels of ADP concentration in surrounding solution. Simulation results obtained for the five parameter sets (see *legend at upper right* for parameter set index) are close to the measured data (*black dots*). Experimental data from Barbour et al. (1984).

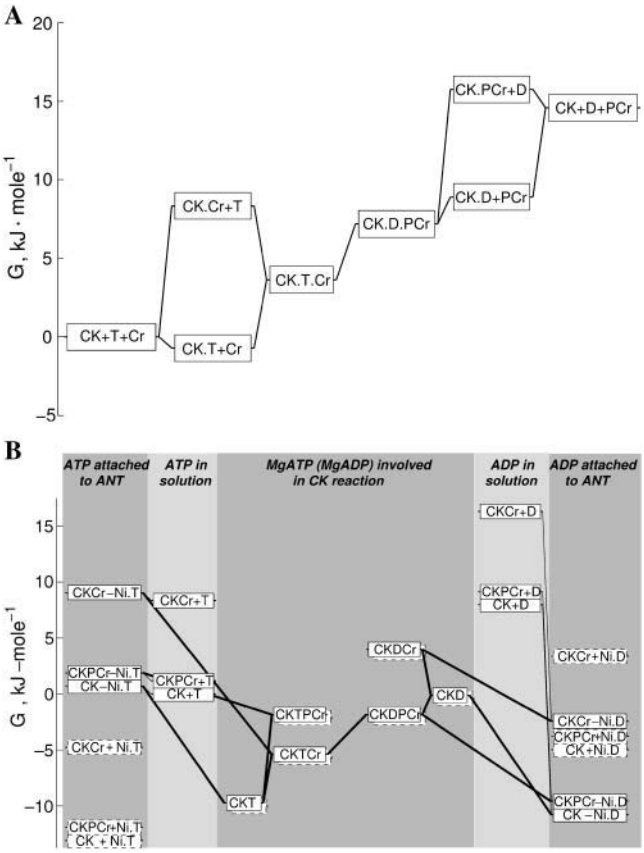

FIGURE 10 The free energy profile of the MiCK reaction in the absence (*subplot A*) or presence (*subplot B*) of oxidative phosphorylation. Note that the free energies of the states are shown relative to different initial states in these schemes: MiCK without any substrates bound and with $MgATP^{2-}$ and Cr in solution (*uncoupled case*); MiCK-ANT complex without any bound substrates, ANT directed toward the intermembrane space, and with Mg^{2+}, Mg-free ATP^{4-}, and Cr in solution (*coupled case*). Such difference in selection of initial states of reactions is due to the difference in the forms of ATP binding to MiCK and ANT: MiCK binds $MgATP^{2-}$ and ANT binds Mg-free ATP^{4-}. (*Subplot A*) The relative free energies of MiCK states are estimated from measured kinetic constants. Here, MgATP and MgADP are denoted as *T* and *D*, respectively. Note that the free energy change during reaction is clear from the difference in free energies after (*CK+D+PCr*) and before (*CK+T+Cr*) the reaction. The differences in maximal rates of forward and backward MiCK reactions can be explained by the differences in the free energies of CK.T.Cr and CK.D.PCr (Eqs. 21–22). (*Subplot B*) Partial free energy profile of the MiCK reaction coupled to ANT. The free energies of the coupled system (*boxes with solid border*) are compared with the free energies of uncoupled MiCK and ANT (*boxes with dashed border*). In the first column, three states of two-protein complexes are shown with ATP (*T* in the scheme) attached to ANT directed to intermembrane space (*Ni*). The total free energy of the MiCK-ANT complex depends on the state of the coupled MiCK, as shown in the first column. ATP, attached to ANT, is either released to solution (*second column*) or transferred from ANT to MiCK (*third column*). After the MiCK reaction, ADP (*D* in the scheme) is transferred to ANT (*last column*) and then either released to solution (*fourth column*) or transported to mitochondrial matrix (*not shown*). This profile corresponds to the parameter set *4* (see Table 3). In the scheme, all reactions that are in the pathway leading to synthesis of PCr after the transfer of ATP from ANT to MiCK are shown by thick lines. Note that there are several simplifications made to keep the profile as simple as possible. First, the free energies changes indicated in the profile are induced by differences of the free energies of the complex states as well as changes in solution due to binding and release of the substrates and magnesium. However, in the scheme, only release and binding of ATP and ADP are indicated. Second, possible binding of ATP and ATP by ANT during the MiCK reaction is not indicated in this profile.

and the free energies after transport of ADP^{3-} to ANT are slightly dropped. Due to such changes, the synthesis of PCr from ATP that is transferred from mitochondrial matrix by ANT becomes energetically advantageous. The net free energy change during the transfer of ATP^{4-} from ANT to MiCK, MiCK reaction, and the transfer of ADP^{3-} from MiCK back to ANT, is negative and ranges from -3.7 kJ mol^{-1} to -20.7 kJ mol^{-1}, depending on the states of MiCK-ANT complex at the beginning and end of the coupled reaction along the main pathway (*thick lines* in the scheme). Note that if the free energies of MiCK-ANT states would be kept the same as in the uncoupled case, then the corresponding net free energy difference would be from -0.3 kJ mol^{-1} to $+16.7$ kJ mol^{-1} (see *boxes with dashed borders* in Fig. 10 *B*).

DISCUSSION

According to our analysis, the simplest kinetic scheme that can reproduce the experimental measurements on functional coupling between mitochondrial creatine kinase (MiCK) and adenine nucleotide translocase (ANT) involves the direct transfer of ATP and ADP between the proteins. The model composed on the basis of the dynamic compartmentation mechanism of functional coupling of MiCK and ANT was not sufficient to reproduce the measured values of apparent dissociation constants of the MiCK reaction (Fig. 3). However, when one assumes the direct transfer of ATP and ADP between MiCK and ANT, it is possible to reproduce the measured kinetic properties of MiCK (Fig. 7) and the estimated direct flux of ADP between MiCK and ANT (Figs. 8 and 9). Direct transfer of ATP and ADP between MiCK and ANT was analyzed by composing free energy profiles of the reactions using a thermodynamically consistent model. To our knowledge, it is the first time that this approach was used to study interactions between MiCK and ANT. Earlier, the analysis based on free energy profiles of reactions was successfully applied in the studies of several biological systems such as mitochondrial inner membrane carriers (Kramer, 1994) and actomyosin cross-bridges in skeletal and heart muscles (Cooke et al., 1994; Eisenberg et al., 1980; Hill, 1974; Vendelin et al., 2000a). Our analysis of the direct transfer mechanism revealed that:

1. The mere establishment of direct transfer between ANT and MiCK, as well as limitation of ATP and ADP release by the proteins, was not sufficient to reproduce the measurements.
2. The measurements can be reproduced if, at least, the free energy of the ANT state with the ANT binding site

directed toward the intermembrane space with ATP attached (state ANT_i.ATP) is changed (Table 2).

Thus, the free energies of several states in coupled MiCK-ANT system are modified to facilitate synthesis of PCr from ATP transported by ANT from mitochondrial matrix to intermembrane space (Fig. 10 *B*).

The mechanism of functional interaction between MiCK and ANT, as suggested by our results, is in accord with the measurements of MiCK kinetics on intact mitochondria in isotonic KCl solution (Kuznetsov et al., 1989). Kuznetsov and co-workers (1989) showed that, after detachment of MiCK from the mitochondrial inner membrane, the influence of oxidative phosphorylation on MiCK reaction kinetics disappears—despite the presence of MiCK in the intermembrane space and the intactness of the mitochondrial outer membrane.

Dynamic compartmentation hypothesis

Gellerich et al. (1987) was able to reproduce, with a simple mathematical model, the inhibition of MiCK-activated mitochondrial respiration by the concurrent ATP-regenerating system. The authors assumed that the diffusion of ADP and ATP between the compartment and the surrounding solution is limited, and that this limitation is the same for both metabolites. This result was confirmed by our model: it is possible to find from such exchange coefficients for ADP and ATP that the exogenously added ATP-regenerating system is inhibiting mitochondrial respiration by $\sim$60% (Fig. 5). Additionally, the model based on the dynamic compartmentation hypothesis was able to reproduce reversal of the MiCK reaction after coupling to oxidative phosphorylation in certain conditions (Fig. 4), even if the exchange coefficients for ADP and ATP are the same as considered by Gellerich et al. (1987).

To check whether the dynamic compartmentation mechanism can reproduce changes in the apparent kinetic constants of the MiCK reaction when coupled to oxidative phosphorylation, we had to extend the original model of Gellerich et al. (1987) by adding more degrees of freedom to the model. Namely, we added ATPase activity into the surrounding solution as well as considering ADP and ATP exchange coefficients independent from each other. These changes were introduced into the model to create large concentration differences between the compartment and the surrounding solution (see Results, Eq. 29). Without these changes, assuming that ADP and ATP exchange coefficients are, for example, the same, neither of the computed apparent coefficients K_a and K_{ia} were reduced by $>\sim$1% from the values measured in the uncoupled case, regardless of the exchange coefficients ($D_{ATP} = D_{ADP}$) used, the ATPase activities in the solution, and the ANT activity used (results not shown). Thus, these extensions of the original model of Gellerich et al. (1987) were the required ones if the reduction of apparent kinetic constants in the model of the coupled MiCK-ANT interaction is desired (Fig. 2). However, even with these extensions, it is impossible to fit the measured dissociation constants K_a and K_{ia} with the model simultaneously (Fig. 3). Thus, the mechanism of dynamic compartmentation is not sufficient to reproduce the measured changes in the apparent kinetic constants of the MiCK reaction coupled to oxidative phosphorylation in isolated heart mitochondria (Jacobus and Saks, 1982; Kuznetsov et al. (1989) and in inner membrane-matrix preparation (Saks et al., 1985).

Direct transfer hypothesis

When the direct transfer between MiCK and ANT is assumed as a basic mechanism of the coupling, it is possible to reproduce the measured kinetic properties of MiCK as well as the estimated direct flux of ADP between MiCK and ANT. Our model was able to reproduce the measurements only if, in addition to the limitation of ATP and ADP release from the MiCK-ANT complex, the free energy of the ANT state with the ANT binding site directed toward the intermembrane space with ATP attached (state ANT_i.ATP) was changed (Table 2). Thus, the mere establishment of direct transfer between ANT and MiCK, as well as limitation of ATP and ADP release by the proteins, was not sufficient to reproduce the measurements, and the free energy profile of MiCK-ANT interaction had to be modified further. The elevation of the free energy of the ANT_i.ATP state proposed by the model is the main result obtained from the analysis of the free energy profile of the coupled MiCK reaction. As it is clear from the free energy profile (Fig. 10 *B*), the MiCK reaction is driven toward synthesis of PCr by altering the free energy of ANT_i.ATP. Note that such increase of the free energy of intermediate state ANT_i.ATP does not inhibit transport of ATP^{4-} from the matrix to the inner membrane space by ANT due to the large differences in the free energies of ATP^{4-} in the intermembrane space and the mitochondrial matrix induced by mitochondrial potential (Klingenberg, 1985). Indeed, we assumed in our model that during a transport of ATP^{4-} from matrix to inner membrane space a net negative charge is transported, close to the estimation by Gropp et al. (1999). With the membrane potential taken equal to -180 mV, the membrane potential contributes $\sim$17 kJ mol^{-1} of the free energy change during a transport of ATP^{4-} from the matrix solution to the inner membrane space solution. In the model, this was accounted for by increasing the free energy of ATP^{4-} in the matrix as well as the free energy of the ANT_x.ATP state by the contribution of membrane potential. Thus, even after increase of the free energy of the intermediate state of ATP^{4-} transport (ANT_i.ATP) by $\sim$13.5 kJ mol^{-1}, the transition from ANT_x.ATP to ANT_i.ATP was still energetically advantageous, and ATP^{4-} transport was not greatly inhibited in the model.

Aliev and Saks (1993, 1994) composed a mathematical model of functional coupling of MiCK and ANT using

a probability approach. In this model, the probabilities of changes in the MiCK-ANT complex states were estimated and the MiCK rate was computed. The computed apparent kinetic constants of the MiCK reaction were close to those actually measured and, in addition, the influence of oxidative phosphorylation on the direction of the MiCK reaction was reproduced (Aliev and Saks, 1993, 1994). According to Aliev and Saks (1993, 1994), the dissociation of ATP and ADP from the MiCK-ANT complex was not greatly limited and dissociation constants of ANT and MiCK were not altered. However, in the derivation of the MiCK reaction rate equation, it was assumed that after transfer of ATP from ANT to MiCK and formation of the ternary complex CK.ATP.Cr, the latter was always utilized in the MiCK reaction (Aliev and Saks, 1993, 1994). This means that either ATP was not allowed to dissociate from the ternary complex, or that the ternary complex was quickly utilized to form an intermediate state of MiCK and the reverse reaction of the latter transformation was not accounted for. Analysis of the free energy profiles carried out in our work (Fig. 10 *B*) shows that the reason for effective synthesis of PCr in the coupled system of MiCK-ANT may be not the accelerated conversion of the central complex CK.ATP.Cr, but the increased free energy of the step preceding the formation of this complex, the free energy of the state ANT_i.ATP.CK, and a decrease of the free energy of the state with the reaction product ANT_i.ADP.CK. The mechanism proposed in our work does not require strong changes in the free energy profile of the reaction of phosphate transfer itself and, thus, develops further the earlier models of direct channeling to explain the acceleration of PCr synthesis by oxidative phosphorylation in a thermodynamically consistent way as well as clarifying the kinetic scheme for further analysis. The molecular nature of this direct transfer remains to be clarified.

Model simplifications

There are three important simplifications introduced into our model of direct transfer:

First, since it is still not clear whether ANT translocates the adenine nucleotides simultaneously (Duyckaerts et al., 1980) or according to the ping-pong mechanism (Brustovetsky et al., 1996; Gropp et al., 1999; Klingenberg, 1989), we had to reduce the dependency of the simulations on the particular type of ANT kinetic scheme as much as possible. This was done by assuming that the elementary steps of ATP and ADP translocation are considerably faster than the MiCK reaction rate. Thus, in our analysis, ANT never limited the coupled MiCK reaction and the predictions of our model can be influenced by this. In other words, it is possible that the mere elevation of the free energy of the ANT_i.ATP state is not sufficient to reproduce the measured kinetic data of the MiCK reaction if the realistic rates of ANT state transformations would be taken into account.

Our second assumption was that ATP and ADP are not released from MiCK after direct transfer of ATP or ADP from ANT. This simplification allowed us to reduce the number of parameters describing ATP and ADP dissociation from the coupled MiCK-ANT complex from 4 to 2 (the free energies of transition $\Delta G^{\ddagger}$ for ATP and ADP release by ANT), which further decreased the number of computations required in the analysis of the MiCK reaction kinetics (Table 2). Note that, alternatively, one can assume that ATP and ADP are released through MiCK only and there is no direct exchange between ANT and solution. However, in the latter case, the model would not be able to simulate uncoupled ANT and MiCK since direct transfer between the proteins would be required for ANT function.

According to our third assumption, MiCK and ANT coupling was induced by interaction between pairs of ANT and MiCK. These pairs were fixed and the direct transfer between ANT and MiCK in different pairs was not considered. Implications of such transfer as well as possibilities of cooperativity between different MiCKs, if one considers MiCK as an octamer (Wallimann et al., 1992) in the kinetics of the MiCK reaction coupled to oxidative phosphorylation, were not studied by us. However, one can use our approach and compose the corresponding kinetic scheme together with the free energy profiles if the experimental data pointing to such an interaction will be found.

Computationally effective phenomenological models

In the development of integrated models of energy transfer, the dynamic compartmentation hypothesis turned out to be very useful for describing the functional coupling between MiCK and ANT phenomenologically. Indeed, when the energy fluxes in the heart cells are modeled and there is no intention to investigate the mechanism of the functional coupling itself, rather simple models of the coupling can be designed (Saks et al., 2000, 2003; Vendelin et al., 2000b). In these models, the equations describing MiCK and ANT interactions were derived on the basis of the dynamic compartmentation hypothesis and then all constants were formally obtained by fitting available experimental data. As a result, simple and computationally effective models were obtained that provide the same MiCK reaction rate as predicted on the basis of the experiments. However, all the obtained constants were apparent ones and these constants, as well as the equations used, are *phenomenological* only and cannot be used to investigate the mechanism of the

functional coupling between MiCK and ANT. For example, the phenomenological constants found by fitting do not obey the Haldane relationship, and thus are not related to the MiCK reaction mechanism (Saks et al., 2003; Vendelin et al., 2000b).

Physiological relevance

There is accumulating evidence to indicate that the intracellular environment is not an aqueous solution of metabolites, but rather a highly organized system with specific intracellular structures and tight interactions between enzymes and organelles as well as a compartmentalization of metabolites (Abraham et al., 2002; Fulton, 1982; Kaasik et al., 2001; Ovadi, 1995; Ovadi and Srere, 1996; Pollack, 2001; Saks et al., 1994; Weiss and Korge, 2001). As a part of this complex intracellular organization, functional coupling between MiCK and ANT plays an important role in regulation of oxidative phosphorylation and maintaining metabolic stability of the heart muscle (Joubert et al., 2002, 2004; Ovadi and Saks, 2004; Saks et al., 2004; Vendelin et al., 2000b). Recently, a protective role of coupling against the opening of the mitochondrial permeability transition pore has been demonstrated by Dolder et al. (2003). Even in the absence of adenine nucleotides in the solution surrounding mitochondria, Cr was able to suppress opening of the mitochondrial permeability transition pore if active MiCK is positioned in the intermembrane space (Dolder et al., 2003).

Since our aim was to describe the phenomenon of functional interactions between MiCK and ANT observed in isolated mitochondria in vitro using the simplest scheme possible, we did not combine the two models used in this study, as the model using direct transfer hypothesis was sufficient to reproduce the experimental data. The mixed model of functional coupling including the two mechanisms—direct transfer of metabolites between the proteins and dynamic compartmentation—is probably the best in describing the situation in vivo. Indeed, when the in vivo environment is mimicked by adding macromolecules to the solution, the diffusion restriction imposed by the mitochondrial outer membrane increases significantly (Gellerich et al., 1994, 2002; Laterveer et al., 1996). Further, the studies on skinned cardiac fibers have confirmed the limited permeability of the mitochondrial outer membrane, among several other distinct diffusion restrictions within the cell (Saks et al., 2003; Vendelin et al., 2004). Thus, the situation in vivo is very different from that in vitro with the mitochondrial outer membrane playing an important role in the regulation of oxidative phosphorylation and the functional coupling between MiCK and ANT is amplified by dynamic compartmentation of metabolites in intermembrane space. For example, in permeabilized muscle fibers, ADP produced by MiCK in the vicinity of ANT is not accessible to the external ADP-trapping system due to the functional coupling between MiCK and ANT (through direct transfer as our results suggest) and, additionally, dynamic compartmentation of the metabolites induced by restricted permeability of mitochondrial outer membrane (Saks et al., 2003). The first steps in the modeling of functional coupling between MiCK and ANT in vivo have already been performed by using the phenomenological approach (Saks et al., 2003, 2004; Vendelin et al., 2000b). The comprehensive model involving the detailed description of direct transfer and dynamic compartmentation to study the interplay between the two mechanisms awaits its further development. Such a model is needed to describe quantitatively the molecular mechanism of the regulation of mitochondrial oxidative phosphorylation under normal and pathological conditions.

APPENDIX

In this Appendix, the model of direct transfer of ATP and ADP between creatine kinase and adenine nucleotide translocase is described. First, we explain how the system of equations was derived. Second, the values of model parameters are given.

System of equations

The model consists of a system of ordinary differential equations. Each differential equation describe changes in a state of MiCK-ANT complex by tracking all fluxes that are connected with the state. States of MiCK-ANT complex are composed from all combinations of one MiCK and one ANT state. The following MiCK states are included in the model:

- MiCK free from all substrates.
- MiCK in binary complex with ATP, ADP, PCr, and Cr—CK.ATP, CK.ADP, CK.PCr, and CK.Cr.
- MiCK in ternary complexes CK.ATP.Cr, CK.ADP.PCr, CK.ADP.Cr, and CK.ATP.PCr.
- MiCK in binary and ternary complexes tightly coupled to ANT (Fig. 1 *B*)—CK_c.ATP, CK_c.ADP, CK_c.ATP.Cr, CK_c.ADP.PCr, CK_c.ADP.Cr, and CK_c.ATP.PCr.

The states of ANT included in the model are:

- Free ANT_i and ANT_x directed toward intermembrane space and mitochondrial matrix, respectively.
- ANT with ATP or ADP bound with ANT directed toward intermembrane space—ANT_i.ATP and ANT_i.ADP.
- ANT with ATP or ADP bound with ANT directed toward mitochondrial matrix—ANT_x.ATP and ANT_x.ADP.

Thus, the total number of tracked states is 90, or 15 MiCK states $\times$ 6 ANT states. In our simulations, all differential equations were integrated until steady state was reached, rendering the distribution of MiCK and ANT states and thereby the corresponding rates of MiCK and ANT reactions.

As an example of the equations used, let us consider the dynamics of the ANT_i-CK_c.ATP state. The processes that lead to this state are as follows. First, ANT_i-CK_c.ATP is formed from ANT_i.ATP-CK during direct transfer of ATP from ANT to MiCK. Second and third, the complex ANT_i-CK_c.ATP is formed after detachment of ATP or ADP from complexes ANT_i.ATP-CK_c.ATP and ANT_i.ADP-CK_c.ATP, respectively. Finally, ANT_i-CK_c.ATP is produced after detachment of PCr or Cr from ANT_i-CK_c.ATP.PCr and ANT_i-CK_c.ATP.Cr, respectively. All processes in the model are reversible according to the principle of microscopic reversibility. Thus, the complex ANT_i-CK_c.ATP can be utilized either in direct transfer of ATP from MiCK to ANT, in binding of ATP and ADP by ANT_i, and in binding of PCr and Cr by CK_c. In sum, for ANT_i-CK_c.ATP we have

$$\frac{d[ANT_i - CK_c.ATP]}{dt} = \nu_{ANT_i.ATP-CK \rightarrow ANT_i-CK_c.ATP} + \nu_{ANT_i.ATP-CK_c.ATP \rightarrow ANT_i-CK_c.ATP} + \nu_{ANT_i.ADP-CK_c.ATP \rightarrow ANT_i-CK_c.ATP} + \nu_{ANT_i-CK_c.ATP.PCr \rightarrow ANT_i-CK_c.ATP} + \nu_{ANT_i-CK_c.ATP.Cr \rightarrow ANT_i-CK_c.ATP} - \nu_{ANT_i-CK_c.ATP \rightarrow ANT_i.ATP-CK} - \nu_{ANT_i-CK_c.ATP \rightarrow ANT_i.ATP-CK_c.ATP} - \nu_{ANT_i-CK_c.ATP \rightarrow ANT_i.ADP-CK_c.ATP} - \nu_{ANT_i-CK_c.ATP \rightarrow ANT_i-CK_c.ATP.PCr} - \nu_{ANT_i-CK_c.ATP \rightarrow ANT_i-CK_c.ATP.Cr}, \quad (A1)$$

where the rate $v_{A \rightarrow B}$ corresponds to the rate of transformation of the MiCK-ANT complex from state A to state B, and $[ANT_i\text{-}CK_c.ATP]$ denotes the relative concentrations of the corresponding MiCK-ANT complex state. The rates of all these individual processes are described by equations similar to Eqs. 23–25 (see Methods). By grouping the rates according to reversible processes and taking into account that the free energy of the MiCK-ANT complex is a sum of free energies of MiCK and ANT states in our model, we obtain the following equations. The rates corresponding to direct transfer of ATP between the proteins are

$$\nu_{ANT_i.ATP-CK \rightarrow ANT_i-CK_c.ATP} = [ANT_i.ATP - CK]\ [Mg^{2+}]\ \alpha\ \exp\left(\frac{-\Delta G_1^{\ddagger}}{RT}\right), \quad (A2)$$

$$\nu_{ANT_i-CK_c.ATP \rightarrow ANT_i.ATP-CK} = [ANT_i - CK_c.ATP]\ \alpha\ \exp\left(\frac{G_{ANT_i} + G_{CK_c.ATP} - G_{ANT_i.ATP} - G_{CK} - G_{Mg} - \Delta G_1^{\ddagger}}{RT}\right), \quad (A3)$$

where $\Delta G_1^{\ddagger}$ is the free energy of transition of the transfer. The rates of ATP detachment from and binding to ANT are

$$\nu_{ANT_i.ATP-CK_c.ATP \rightarrow ANT_i-CK_c.ATP} = [ANT_i.ATP - CK_c.ATP]\ \alpha\ \exp\left(\frac{G_{ANT_i.ATP} - G_{ANT_i} - G_{fATP} - \Delta G_2^{\ddagger}}{RT}\right), \quad (A4)$$

$$\nu_{ANT_i-CK_c.ATP \rightarrow ANT_i.ATP-CK_c.ATP} = [ANT_i - CK_c.ATP]\ [fATP]\ \alpha\ \exp\left(\frac{-\Delta G_2^{\ddagger}}{RT}\right), \quad (A5)$$

where $\Delta G_2^{\ddagger}$ is the free energy of transition of ATP attachment to ANT and fATP corresponds to Mg^{2+}-free form of ATP. The rates of ADP detachment from and binding to ANT are

$$\nu_{ANT_i.ADP-CK_c.ATP \rightarrow ANT_i-CK_c.ATP} = [ANT_i.ADP - CK_c.ATP]\ \alpha\ \exp\left(\frac{G_{ANT_i.ADP} - G_{ANT_i} - G_{fADP} - \Delta G_3^{\ddagger}}{RT}\right), \quad (A6)$$

$$\nu_{ANT_i-CK_c.ATP \rightarrow ANT_i.ADP-CK_c.ATP} = [ANT_i - CK_c.ATP]\ [fADP]\ \alpha\ \exp\left(\frac{-\Delta G_3^{\ddagger}}{RT}\right), \quad (A7)$$

where $\Delta G_3^{\ddagger}$ is the free energy of transition of ATP attachment to ANT, and fADP corresponds to the Mg^{2+}-free form of ADP. Similar rate equations describe the formation of MiCK ternary complexes and reduction of ternary complexes to binary complexes: PCr detachment and attachment,

$$\nu_{ANT_i-CK_c.ATP.PCr \rightarrow ANT_i-CK_c.ATP} = [ANT_i - CK_c.ATP.PCr]\ \alpha\ \exp\left(\frac{G_{CK_c.ATP.PCr} - G_{CK_c.ATP} - G_{PCr} - \Delta G_4^{\ddagger}}{RT}\right), \quad (A8)$$

$$\nu_{ANT_i-CK_c.ATP \rightarrow ANT_i-CK_c.ATP.PCr} = [ANT_i - CK_c.ATP]\ [PCr]\ \alpha\ \exp\left(\frac{-\Delta G_4^{\ddagger}}{RT}\right), \quad (A9)$$

as well as Cr detachment and attachment,

$$\nu_{ANT_i-CK_c.ATP.Cr \rightarrow ANT_i-CK_c.ATP} = [ANT_i - CK_c.ATP.Cr]\ \alpha\ \exp\left(\frac{G_{CK_c.ATP.Cr} - G_{CK_c.ATP} - G_{Cr} - \Delta G_5^{\ddagger}}{RT}\right), \quad (A10)$$

$$\nu_{ANT_i-CK_c.ATP \rightarrow ANT_i-CK_c.ATP.Cr} = [ANT_i - CK_c.ATP]\ [Cr]\ \alpha\ \exp\left(\frac{-\Delta G_5^{\ddagger}}{RT}\right). \quad (A11)$$

The free energies of transition $\Delta G_4^{\ddagger}$ and $\Delta G_5^{\ddagger}$ correspond to attachment of PCr and Cr, respectively.

During titration with ATP in the presence of Cr, ADP is produced by MiCK. Part of this ADP is going into mitochondrial matrix directly after a transfer between MiCK and ANT. Another part is released into solution, either by ANT after the direct transfer (Fig. 1 *B*) or produced in MiCK reaction from ATP according to a random Bi-Bi type mechanism (Fig. 1 *A*). Thus, we have to include in the model the equation describing ADP concentration as well. This was done by composing a differential equation, which describes ADP concentration changes in the solution, induced by either release of ADP from MiCK-ANT complex to the intermembrane space or binding of ADP from the intermembrane space to MiCK-ANT complex. To keep the model simple, ATP concentration in solution was fixed.

For simplicity, ATP synthesis from ADP in matrix was modeled by setting ANT_x.ATP and ANT_x.ADP equal to 90% and 10% of total ANT directed toward mitochondrial matrix, respectively (Aliev and Saks, 1994). Mitochondrial inner membrane potential was taken equal to −180 mV.

The model was further extended to reproduce the studies on radioactively labeled adenine nucleotide uptake in the presence of MiCK activity (Barbour et al., 1984). Namely, radioactivity of all MiCK-ANT complex states with bound adenine nucleotides was tracked by a separate system of linear ordinary differential equations. When more than one adenine nucleotide was bound to the state of the MiCK-ANT complex, radioactivity of each of them was tracked separately, rendering the number of equations in the aforementioned system equal to 132. The simulations were performed as follows: First, the steady-state distribution of MiCK-ANT complex among all states was computed as in all other simulations. Second, the result of the first step (distribution of MiCK-ANT states and rates of transitions from one

state to another) was used for computing the fluxes of radioactive adenine isotopes between the states of the MiCK-ANT complex.

Parameter values

The precise values of selected free energies of Mg^{2+}, PCr, Cr, and forms of ATP and ADP are of no importance in the derived equations, as long as the free energy changes in reactions (the MiCK reaction and Mg^{2+} association with ATP and ADP) are considered and the free energies of the MiCK and ANT states are derived from kinetic measurements using predescribed free energies of the substrates. The free energy change in MgATP+Cr $\rightarrow$ MgADP+PCr reaction is $\sim$14.6 kJ mol^{-1} at 25°C and pH = 7.1 (Golding et al., 1995; Teague and Dobson, 1992; Teague et al., 1996). The relative free energies of Mg^{2+} as well as Mg^{2+}-free ATP and ADP were taken equal to 7.44 kJ mol^{-1}, 0 kJ mol^{-1}, and 0 kJ mol^{-1}, respectively (free energies of ADP and ATP were fixed at zero level). Taking into account that Mg^{2+} dissociation constants for MgATP and MgADP are 24 μM and 347 μM, free energies of MgATP and MgADP are equal to -1.81 kJ mol^{-1} and 4.81 kJ mol^{-1}, respectively. On the basis of these free energies and free energy change during MiCK reaction, we took the relative free energy of PCr equal to 3.98 kJ mol^{-1} and that of Cr equal to -3.98 kJ mol^{-1}.

The free energies of uncoupled MiCK states were derived using the kinetic constants from Aliev and Saks (1997) and Jacobus and Saks (1982). Taking the free energy of MiCK without any substrates attached equal to 0 kJ mol^{-1}, the following free energies were found: $G_{CK.ATP} = -2.52$ kJ mol^{-1}, $G_{CK.ADP} = -0.87$ kJ mol^{-1}, $G_{CK.Cr} = -4.35$ kJ mol^{-1}, $G_{CK.PCr} = 5.15$ kJ mol^{-1}, $G_{CK.ATP.Cr} = -2.16$ kJ mol^{-1}, $G_{CK.ADP.PCr} = 1.40$ kJ mol^{-1}, $G_{CK.ADP.Cr} = -0.76$ kJ mol^{-1}, and $G_{CK.ATP.PCr} = 9.34$ kJ mol^{-1}.

The free energies of ANT states were derived, assuming a 5 μM dissociation constant for binary complex of ANT with both Mg^{2+}-free ATP and ADP either in the intermembrane space or in the matrix. Taking free energy of ANT without any substrates attached equal to 0 kJ mol^{-1}, free energies of ANT states associated with ATP or ADP are both taken equal to -13.13 kJ mol^{-1} provided that the mitochondrial membrane potential is zero. Assuming that only during ATP transport will a net charge be transported, the mitochondrial membrane potential contributed to the increase in the free energy of ATP in the matrix and that of the ANT binary complex, facing mitochondrial matrix with ATP attached.

All reactions in the system were given rates relative to the MiCK reaction in direction of PCr production. Namely, the reaction rate constant for CK.ATP.Cr $\rightarrow$CK.ADP.PCr transformation was taken equal to 1 s^{-1}. Since we used a factor $\alpha = 10^6$ (see Eqs. 23–25 in Methods), the free energy of transition for this transformation was taken equal to 34.25 kJ mol^{-1}. In the uncoupled system, the attachment and detachment of substrates was assumed to be almost in equilibrium with the free energy of transition for attachment of substrates taken equal to $\Delta G^{\ddagger} = 1$ kJ mol^{-1}.

The free energies of transition for ATP and ADP transport by ANT from intermembrane space to matrix was taken equal to 28.54 kJ mol^{-1} leading to a transport rate constant 10 times larger than that for the CK.ATP.Cr $\rightarrow$ CK.ADP.PCr reaction. By using these relatively large rate constants for ATP and ADP transport by ANT, we ensured that none of the studied mechanisms of MiCK and ANT coupling were limited by ANT transport and thereby not ruled out due to underestimation of these rate constants.

In the system coupled via direct transfer, the free energies of transition for some reactions was changed as explained in Methods and Results.

We thank Prof. Marc Jamin (Laboratoire de Biophysique Moléculaire et Cellulaire, Commissariat à l'Energie Atomique-Grenoble, Grenoble, France) and Prof. Jüri Engelbrecht (Institute of Cybernetics at Tallinn Technical University, Estonia) for interesting discussions and comments on the manuscript.

This work was supported in part by the Marie Curie Fellowship of the European Community program ''Improving Human Research Potential and the Socioeconomic Knowledge Base'' (contract HPMF-CT-2002-01914 to M.V.) and the Estonian Science Foundation (grant 4704).

REFERENCES

Abraham, M. R., V. A. Selivanov, D. M. Hodgson, D. Pucar, L. V. Zingman, B. Wieringa, P. P. Dzeja, A. E. Alekseev, and A. Terzic. 2002. Coupling of cell energetics with membrane metabolic sensing. Integrative signaling through creatine kinase phosphotransfer disrupted by M-CK gene knock-out. *J. Biol. Chem.* 277:24427–24434.

Aliev, M. K., and V. A. Saks. 1993. Quantitative analysis of the ''phosphocreatine shuttle.'' I. A probability approach to the description of phosphocreatine production in the coupled creatine kinase-ATP/ADP translocase-oxidative phosphorylation reactions. *Biochim. Biophys. Acta.* 1143:291–300.

Aliev, M. K., and V. A. Saks. 1994. Mathematical modeling of intracellular transport processes and the creatine kinase systems: a probability approach. *Mol. Cell. Biochem.* 133–134:333–346.

Aliev, M. K., and V. A. Saks. 1997. Compartmentalized energy transfer in cardiomyocytes: use of mathematical modeling for analysis of in vivo regulation of respiration. *Biophys. J.* 73:428–445.

Barbour, R. L., J. Ribaudo, and S. H. Chan. 1984. Effect of creatine kinase activity on mitochondrial ADP/ATP transport. Evidence for a functional interaction. *J. Biol. Chem.* 259:8246–8251.

Bessman, S. P., and A. Fonyo. 1966. The possible role of the mitochondrial bound creatine kinase in regulation of mitochondrial respiration. *Biochem. Biophys. Res. Commun.* 22:597–602.

Bessman, S. P., and P. J. Geiger. 1981. Transport of energy in muscle: the phosphorylcreatine shuttle. *Science.* 211:448–452.

Brown, P. N., G. D. Byrne, and A. C. Hindmarch. 1989. VODE: a variable coefficient ODE solver. *SIAM J. Sci. Stat. Comput.* 10:1038–1051.

Brustovetsky, N., A. Becker, M. Klingenberg, and E. Bamberg. 1996. Electrical currents associated with nucleotide transport by the reconstituted mitochondrial ADP/ATP carrier. *Proc. Natl. Acad. Sci. USA.* 93:664–668.

Cooke, R., H. White, and E. Pate. 1994. A model of the release of myosin heads from actin in rapidly contracting muscle fibers. *Biophys. J.* 66: 778–788.

Dolder, M., B. Walzel, O. Speer, U. Schlattner, and T. Wallimann. 2003. Inhibition of the mitochondrial permeability transition by creatine kinase substrates. Requirement for microcompartmentation. *J. Biol. Chem.* 278: 17760–17766.

Duyckaerts, C., C. M. Sluse-Goffart, J. P. Fux, F. E. Sluse, and C. Liebecq. 1980. Kinetic mechanism of the exchanges catalysed by the adenine-nucleotide carrier. *Eur. J. Biochem.* 106:1–6.

Dzeja, P. P., and A. Terzic. 2003. Phosphotransfer networks and cellular energetics. *J. Exp. Biol.* 206:2039–2047.

Eisenberg, E., T. L. Hill, and Y. Chen. 1980. Cross-bridge model of muscle contraction. Quantitative analysis. *Biophys. J.* 29:195–227.

Fulton, A. B. 1982. How crowded is the cytoplasm? *Cell.* 30:345–347.

Gellerich, F., and V. A. Saks. 1982. Control of heart mitochondrial oxygen consumption by creatine kinase: the importance of enzyme localization. *Biochem. Biophys. Res. Commun.* 105:1473–1481.

Gellerich, F. N., M. Kapischke, W. Kunz, W. Neumann, A. Kuznetsov, D. Brdiczka, and K. Nicolay. 1994. The influence of the cytosolic oncotic pressure on the permeability of the mitochondrial outer membrane for ADP: implications for the kinetic properties of mitochondrial creatine kinase and for ADP channelling into the intermembrane space. *Mol. Cell. Biochem.* 133–134:85–104.

Gellerich, F. N., F. D. Laterveer, S. Zierz, and K. Nicolay. 2002. The quantitation of ADP diffusion gradients across the outer membrane of heart mitochondria in the presence of macromolecules. *Biochim. Biophys. Acta.* 1554:48–56.

Gellerich, F. N., M. Schlame, R. Bohnensack, and W. Kunz. 1987. Dynamic compartmentation of adenine nucleotides in the mitochondrial intermembrane space of rat-heart mitochondria. *Biochim. Biophys. Acta.* 890:117–126.

Golding, E. M., W. E. Teague, Jr., and G. P. Dobson. 1995. Adjustment of K′ to varying pH and pMg for the creatine kinase, adenylate kinase and

ATP hydrolysis equilibria permitting quantitative bioenergetic assessment. *J. Exp. Biol.* 198:1775–1782.

Gropp, T., N. Brustovetsky, M. Klingenberg, V. Muller, K. Fendler, and E. Bamberg. 1999. Kinetics of electrogenic transport by the ADP/ATP carrier. *Biophys. J.* 77:714–726.

Hill, T. L. 1974. Theoretical formalism for the sliding filament model of contraction of striated muscle. Part I. *Prog. Biophys. Mol. Biol.* 28: 267–340.

Jacobs, H. K., and S. A. Kuby. 1970. Studies on adenosine triphosphate transphosphorylases. IX. Kinetic properties of the crystalline adenosine triphosphate-creatine transphosphorylase from calf brain. *J. Biol. Chem.* 245:3305–3314.

Jacobus, W. E., and A. L. Lehninger. 1973. Creatine kinase of rat heart mitochondria. Coupling of creatine phosphorylation to electron transport. *J. Biol. Chem.* 248:4803–4810.

Jacobus, W. E., and V. A. Saks. 1982. Creatine kinase of heart mitochondria: changes in its kinetic properties induced by coupling to oxidative phosphorylation. *Arch. Biochem. Biophys.* 219:167–178.

Joubert, F., P. Mateo, B. Gillet, J.-C. Beloeil, J.-L. Maznet, and J. A. Hoerter. 2004. CK flux or direct ATP transfer: versatility of energy transfer pathways evidenced by NMR in the perfused heart. *Mol. Cell. Biochem.* 256/257:29–41.

Joubert, F., J. L. Mazet, P. Mateo, and J. A. Hoerter. 2002. ^{31}P NMR detection of subcellular creatine kinase fluxes in the perfused rat heart: contractility modifies energy transfer pathways. *J. Biol. Chem.* 277: 18469–18476.

Kaasik, A., V. Veksler, E. Boehm, M. Novotova, A. Minajeva, and R. Ventura-Clapier. 2001. Energetic crosstalk between organelles: architectural integration of energy production and utilization. *Circ. Res.* 89: 153–159.

Klingenberg, M. 1985. The ADP/ATP carrier in mitochondrial membranes. *In* The Enzymes of Biological Membranes. A. N. Martonosi, editor. Plenum Press, NY. 4:511–553.

Klingenberg, M. 1989. Molecular aspects of the adenine nucleotide carrier from mitochondria. *Arch. Biochem. Biophys.* 270:1–14.

Korzeniewski, B. 1998. Regulation of ATP supply during muscle contraction: theoretical studies. *Biochem. J.* 330:1189–1195.

Kramer, R. 1994. Functional principles of solute transport systems: concepts and perspectives. *Biochim. Biophys. Acta.* 1185:1–34.

Kuznetsov, A. V., Z. A. Khuchua, E. V. Vassil'eva, N. V. Medved'eva, and V. A. Saks. 1989. Heart mitochondrial creatine kinase revisited: the outer mitochondrial membrane is not important for coupling of phosphocreatine production to oxidative phosphorylation. *Arch. Biochem. Biophys.* 268:176–190.

Laterveer, F. D., K. Nicolay, and F. N. Gellerich. 1996. ADP delivery from adenylate kinase in the mitochondrial intermembrane space to oxidative phosphorylation increases in the presence of macromolecules. *FEBS Lett.* 386:255–259.

Morrison, J. F., and E. James. 1965. The mechanism of the reaction catalyzed by adenosine triphosphate-creatine phosphotransferase. *Biochem. J.* 97:37–52.

Moré, J. J., D. C. Sorensen, K. E. Hillstrom, and B. S. Garbow. 1984. The MINPACK project. *In* Sources and Development of Mathematical Software. W. J. Cowell, editor. Prentice-Hall, Englewood Cliffs, NJ.

Ovadi, J. 1995. Cell Architecture and Metabolic Channeling. Springer-Verlag, Heidelberg, Germany.

Ovadi, J., and V. Saks. 2004. On the origin of intracellular compartmentation and organized metabolic systems. *Mol. Cell. Biochem.* 256/257:5–12.

Ovadi, J., and P. A. Srere. 1996. Metabolic consequences of enzyme interactions. *Cell Biochem. Funct.* 14:249–258.

Pollack, G. H. 2001. Cells, Gels and the Engines of Life: A New, Unifying Approach to Cell Function. Ebner & Sons Publishers, Seattle, WA.

Saks, V., A. Kuznetsov, T. Andrienko, Y. Usson, F. Appaix, K. Guerrero, T. Kaambre, P. Sikk, M. Lemba, and M. Vendelin. 2003. Heterogeneity of ADP diffusion and regulation of respiration in cardiac cells. *Biophys. J.* 84:3436–3456.

Saks, V. A., G. B. Chernousova, D. E. Gukovsky, V. N. Smirnov, and E. I. Chazov. 1975. Studies of energy transport in heart cells. mitochondrial isoenzyme of creatine phosphokinase: kinetic properties and regulatory action of Mg^{2+} ions. *Eur. J. Biochem.* 57:273–290.

Saks, V. A., Z. A. Khuchua, E. V. Vasilyeva, O. Y. Belikova, and A. V. Kuznetsov. 1994. Metabolic compartmentation and substrate channelling in muscle cells. Role of coupled creatine kinases in in vivo regulation of cellular respiration—a synthesis. *Mol. Cell Biochem.* 133–134:155–192.

Saks, V. A., O. Kongas, M. Vendelin, and L. Kay. 2000. Role of the creatine/phosphocreatine system in the regulation of mitochondrial respiration. *Acta Physiol. Scand.* 168:635–641.

Saks, V. A., A. V. Kuznetsov, V. V. Kupriyanov, M. V. Miceli, and W. E. Jacobus. 1985. Creatine kinase of rat heart mitochondria. The demonstration of functional coupling to oxidative phosphorylation in an inner membrane-matrix preparation. *J. Biol. Chem.* 260:7757–7764.

Saks, V. A., A. V. Kuznetsov, M. Vendelin, K. Guerro, L. Kay, and E. K. Seppet. 2004. Functional coupling as a basic mechanism of feedback regulation of cardiac energy metabolism. *Mol. Cell. Biochem.* 256/257: 185–199.

Saks, V. A., and R. Ventura-Clapier. editors.1994. Cellular Bioenergetics: Role of Coupled Creatine Kinases. Kluwer Academic Publishers, Boston, MA.

Saks, V. A., R. Ventura-Clapier, Z. A. Khuchua, A. N. Preobrazhensky, and I. V. Emelin. 1984. Creatine kinase in regulation of heart function and metabolism. I. Further evidence for compartmentation of adenine nucleotides in cardiac myofibrillar and sarcolemmal coupled ATPase creatine kinase systems. *Biochim. Biophys. Acta.* 803:254–264.

Seppet, E. 1979. Studies on the mechanisms of phosphocreatine synthesis coupled to glycolytic reactions and mitochondrial oxidative phosphorylation in muscle cells. Ph.D. thesis, Moscow, Russia.

Teague, W. E., Jr., and G. P. Dobson. 1992. Effect of temperature on the creatine kinase equilibrium. *J. Biol. Chem.* 267:14084–14093.

Teague, W. E., Jr., E. M. Golding, and G. P. Dobson. 1996. Adjustment of K′ for creatine kinase, adenylate kinase and ATP hydrolysis equilibria to varying temperature and ionic strength. *J. Exp. Biol.* 199:509–512.

Vendelin, M., P. H. M. Bovendeerd, T. Arts, J. Engelbrecht, and D. H. van Campen. 2000a. Cardiac mechanoenergetics replicated by cross-bridge model. *Ann. Biomed. Eng.* 28:629–640.

Vendelin, M., M. Eimre, E. Seppet, N. Peet, T. Andrienko, M. Lemba, J. Engelbrecht, E. K. Seppet, and V. A. Saks. 2004. Intracellular diffusion of adenosine phosphates is locally restricted in cardiac muscle. *Mol. Cell. Biochem.* 256/257:229–241.

Vendelin, M., O. Kongas, and V. Saks. 2000b. Regulation of mitochondrial respiration in heart cells analyzed by reaction-diffusion model of energy transfer. *Am. J. Physiol. Cell Physiol.* 278:C747–C764.

Wallimann, T., M. Wyss, D. Brdiczka, K. Nicolay, and H. M. Eppenberger. 1992. Intracellular compartmentation, structure and function of creatine kinase isoenzymes in tissues with high and fluctuating energy demands: the ''phosphocreatine circuit'' for cellular energy homeostasis. *Biochem. J.* 281:21–40.

Weiss, J. N., and P. Korge. 2001. The cytoplasm: no longer a well-mixed bag. *Circ. Res.* 89:108–110.